NITRATE EXPORT RESPONSE TO SPATIALLY DISTRIBUTED SNOWMELT IN ALPINE CATCHMENTS

By Danielle Perrot
B.S., Environmental Science, University of California Los Angeles, 2010

A Thesis submitted to the
Faculty of the Graduate School of the
University of Colorado in partial fulfillment
Of the requirement for the degree of
Master of Arts
Department of Geography
2012

This Thesis entitled:

Nitrate export response to spatially distributed snowmelt in alpine catchments

Written by

Danielle O. Perrot

Has been approved for the

Department of Geography

Noah P. Molotch, Chair

Mark W. Williams

Suzanne P. Anderson

Date _____

The final copy of this thesis has been examined by the signatories, and we find that both the content and the form met acceptable presentation standards of scholarly work in the above mentioned discipline

ABSTRACT

Perrot, Danielle O. (M.A. Geography)

Nitrate export response to spatially distributed snowmelt in alpine catchments

Thesis directed by Professor Noah Molotch

This study explores the stream nitrate response to spatially distributed snowmelt in alpine environments. Green Lakes Valley, CO (GLV4) and Tokapah Basin, CA (TOK) are two geologically and climatologically different alpine watersheds that served as our study sites for hydrochemistry comparisons (focused on nitrate, NO_3-) over a 12 year period (1996-2007). A snow water equivalent reconstruction model was used to estimate daily grids of snowmelt and nitrate flushing for each basin. From a nitrate mass balance, I found that GLV4 exhibited high levels of nitrate-export (i.e. greater stream nitrate-export than snowpack nitrate-loading) for all 12 years. In TOK, years with deeper snowpacks exhibited net nitrate-export from the basin, and years with shallower snowpacks exhibited nitrate-retention. Contributing areas of nitrate (i.e. snowpack and soil flushing) were better correlated with the stream nitrate concentration in TOK than in GLV4. In TOK, as much as 76% of the variability in the stream nitrate pulse could be explained by a spatially distributed snowmelt model. In GLV4, on average only 44% of the variability in the stream nitrate pulse could be explained by this spatially distributed snowmelt model. These results suggest that GLV4 may be potentially less sensitive to snowpack N-loading and snowmelt than TOK. As the snowpack regimes of these alpine catchments are altered by climate change and nitrogen-loading to these areas increases over the next century, it will become increasingly important to understand how these fragile ecosystems may react chemically, hydrologically, and ecologically.

ACKNOWLEDGEMENTS

I am extremely grateful towards my advisor Noah Molotch and committee members Mark Williams and Suzanne Anderson for their invaluable guidance and significant contributions to my education. Additional thanks to Noah for his patience, helping me publish my first paper while working on this thesis, and supporting my creativity and ambition. Many thanks to Nel Caine, Jim Sickman, John Melack and countless students for all of their time and hard work in the field to collect detailed the long term observational records of TOK and GLV4. This study would not have been possible without Steve Jepsen's SWE reconstruction modeling work. I am greatly indebted to Mike Gleason, Galen Maclaurin, and Mahsa Moussavi for the crash courses in programming in ENVI and Python for Arc. This thesis would not have been possible without the support of my incredibly intelligent friends, particularly Leah Meromy, Dominik Schneider, Katya Hafich, Morgan Zeliff, Scott Anderson, and Brad Markle. Finally, a huge thank you to Dad for telling me to go to bed, to Rosie for keeping me open-minded, and to Mom for the discussion-talks.

Table of Contents

List of Tables

List of Figures

1. INTRODUCTION

The hydrologic dynamics at play within a watershed may determine its response to changes in climate. Basins that exhibit significant relationships between hydrologic events and stream response may be poorly hydrologically buffered to changes in air temperature and/or the spatiotemporal distribution of precipitation and snowmelt. This could have serious implications not only for hydrologic processes, but also ecology, biogeochemistry, and water resources. This study explored whether variability in the spatiotemporal distribution of snowmelt could explain the variability in stream nitrate concentrations as a means to characterize the hydrochemical sensitivity of alpine catchments.

It is estimated that 1/6 of the world's population is dependent on water originating in mountainous environments in the form of seasonal snowmelt [*Barnett et al.*, 2005; *Bales et al.*, 2006; *Wagener et al.*, 2010]. The seasonal snowpack acts as a natural reservoir that efficiently stores water in its frozen form during the winter months, and releases it to streams and groundwater as temperatures increase during spring and summer [*Mote*, 2006; *Kapnick and Hall*, 2010]. The timing and magnitude of snowmelt is highly sensitive to changes in climate. As temperatures warm, it is expected that a greater percent of mountainous precipitation will fall as rain rather than snow [*Barnett et al.*, 2005; *Bales et al.*, 2006], and that the timing of snowmelt could advance by as much six weeks [*Adam et al.*, 2009; *Magnusson et al.*, 2010].

Alpine environments are not only climatologically sensitive, but also exhibit notable biogeochemical sensitivity [*Brooks and Williams*, 1999; *Fenn et al.*, 2003]. High elevation alpine environments tend to be characterized as "barren" due to low amounts of woody vegetation. Often there is more exposed bedrock, shallower soil depths, and lower soil production rates compared to lower elevation ecosystems. These environments experience nutrient limitations

with regards to phosphorus (P), carbon (C), and nitrogen (N), and are highly sensitive to changes in fluxes of these nutrients due to poorly-buffered soils and surface waters [*Baron et al.*, 1994; *Heuer et al.*, 1999; *Williams and Tonnessen*, 2000]. Atmospheric deposition, hydrologic flushing, microbial activity, and biological assimilation largely govern nutrient cycling in alpine areas.

Nitrogen is an essential building block of life and the primary element present in the atmosphere. Inorganic reactive forms of N (NO_3- and NH_4+) are crucial for biologic activity, fertilizer production, and supporting the food-demand of a growing global population [*Galloway et al.*, 2003]. Nitrogen oxides (NO_x) from combustive reactions, agricultural production of gaseous ammonia, and anthropogenically-produced particulate N reach the atmosphere and result in atmospheric wet (i.e. precipitation) and dry deposition of nitrogen to the land surface [*Williams and Tonnessen*, 2000]. Dissolved inorganic nitrogen (DIN, both nitrate and ammonium) has exhibited an increase in loading to alpine environments, particularly in Europe and the United States [*Dise and Wright*, 1995; *Fenn et al.*, 1998; *Burns*, 2003]. In general, there is little export of nitrate because it is a limiting nutrient. However, there have been reports of N saturation (i.e. net catchment export of N) in the Front Range of the Rocky Mountains in Colorado [*Williams and Tonnessen*, 2000]. Nitrate is a pollutant when it is present in high concentrations in water reservoirs (i.e. streams, lakes, groundwater), resulting in water acidification, eutrophication, and anoxia [*Burns*, 2003; *Gruber and Galloway*, 2008].

The snowpack can act as a nitrate source during the initial snowmelt pulse as it releases its accumulation of atmospherically deposited nitrate (see Background section for further detail on nitrate processes in snow-dominated alpine regions). Enhanced atmospheric deposition of nitrate to alpine environments has increased in the last century partially due to increased

precipitation in higher elevation areas [*Williams et al.*, 1996b] and partially due to increased industrial activity in lower elevation areas [*Williams and Tonnessen*, 2000; *Sickman et al.*, 2002; *Burns*, 2003]. Much of the precipitation in the U.S. Mountain West occurs during the winter months in the form of snow, and hence almost half of nitrate deposition in precipitation occurs during the winter and accumulates in the snowpack [*Williams and Tonnessen*, 2000]. The Niwot Ridge National Atmospheric Deposition Program (NADP) site measured an increase in wet deposition from 1.8 kg ha^{-1} $year^{-1}$ to 4.7 kg ha^{-1} $year^{-1}$ from the mid-1980s to the early 1990s [*Williams et al.*, 1996b; *Burns*, 2003]. The Sierra Nevada also experiences nitrate loading, but to a lesser degree than Niwot Ridge or other alpine catchments in the Colorado Front Range. Williams *et al.* [1996a] reported an average DIN (NH_4+ and NO_3-) loading of 2.53 kg ha^{-1} $year^{-1}$ to a site in Yosemite National Park (CA), and Sickman *et al.* [2001] reported values ranging between 2.0 to 4.9 kg ha^{-1} $year^{-1}$ at Emerald Lake, a subcatchment of the Tokapah basin in Sequoia National Park (CA). Release of nitrate from the snowpack is concentrated in the initial phase of snowmelt due to the ionic pulse [*Johannessen and Henriksen*, 1978], such that the nitrate concentration in the first meltwater leaving the snowpack may be twenty-times greater than the bulk snowpack concentration [*Williams et al.*, 1996c].

Nitrate is prone to flushing from the terrestrial environment during events such as rainfall or snowmelt. However, the addition of water to soils can also increase microbial activity and vegetation assimilation of nitrate. The path of nitrate from the snowpack to the soil, plants, lakes, or streams is complicated by basin topography [*Sickman et al.*, 2002], particularly in environments with large amounts of talus, soil, and/or highly fractured bedrock [*Williams et al.*, 1996b; *Sickman et al.*, 2002; *Liu et al.*, 2004; *Molotch et al.*, 2008; *Cowie et al.*, 2011]. The chemical composition of meltwater end of a flowpath is altered from its original composition

when it left the base of the snowpack [*Campbell et al.*, 1995; *Meixner et al.*, 2000]. It is ultimately the interaction of water with a basin's landscape subunits that determines if, how, and when nitrate will travel from the snowpack to the stream.

Basin landscape subunits (i.e. talus, rock, soil) may vary greatly along hydrologic flowpaths [*Wolford et al.*, 1996; *Meixner et al.*, 2000; *Ross A Wolford*, 2007]. Soils are a dynamic component of N-cycling in alpine environments, acting as a source and/or a sink of nitrate, depending on soil characteristics and productivity. Vegetated soils have the ability to immobilize and assimilate nitrate [*Heuer et al.*, 1999], but are also subject to flushing of inorganic N from rain or snowmelt [*Sickman et al.*, 2001]. Talus may also play an important role as a source of nitrate. Bieber [1998] found that pools of inorganic N in talus were similarly sized to those in nearby alpine soils at Niwot Ridge, CO. However, retention of inorganic N may be greater in soils than talus due to more vegetation and greater biological demand, and therefore greater potential for N-assimilation. Additionally, Campbell *et al.* [1995] argued that shallow groundwater may also play a role in the stream nitrate pulse, as NH_4+ is mineralized and nitrified into NO_3- en route to the shallow groundwater [*Rascher et al.*, 1987], and that this is added to the NO_3- leaving the snowpack and entering the stream, thereby resulting in very high levels of NO_3- in outflow during the first flush. Soil and talus' role as a source or sink of N in alpine environments is largely dependent on their spatial extent, vegetation communities, basin climatology, and hydrologic flowpaths [*Heuer et al.*, 1999; *Sickman et al.*, 2002; *Ley et al.*, 2004; *Molotch et al.*, 2008].

Numerous studies have explored the role of the seasonal snowpack in nitrate dynamics in alpine systems. Sickman *et al.* [2001] found that in the Sierra Nevada, stream nitrate pulses were greater in years with deeper snowpacks that exhibited later melt dates. The authors hypothesized

that this was due to an increase in the size of labile N pools in soils in years with longer snowcover duration. Williams *et al.* [1996] found high amounts of inorganic N present in soils immediately prior to snowmelt at Niwot Ridge, CO, suggesting overwinter subnivial microbial activity. Brooks and Williams [1999] found that winter soil temperature at Niwot Ridge was largely controlled by snow depth with warmer soil temperatures under deeper snowpacks (with insulating depths at approximately 40 cm), which likely resulted in greater overwinter microbial activity that affected the soil as a N source or sink. They also found an inverse relationship between subnivial N-immobilization and N-leachate, such that less N-immobilization and more N-leachate was observed under shallower snowpacks that exhibited periods of snow disappearance during the winter months [*Brooks and Williams*, 1999]. This is the opposite of the results found by Sickman *et al.* [2001], and the disparity between the results of these studies exemplifies the complexity of nitrate and hydrologic cycling within and between basins.

Monitoring seasonal snowpacks is extremely challenging, given the inaccessibility and hostility of alpine environments. Advancements and innovations in remote sensing techniques have improved the monitoring of remote mountainous areas at a finer spatiotemporal scale. Snow covered area (SCA) can now be mapped at the subpixel scale [*Painter et al.*, 2003; 2009], and sensors such as AVHRR (Advanced Very High Resolution Radiometer) and MODIS (Moderate Resolution Imaging Spectroradiometer) provide daily imagery of the land surface. The coupling of remote sensing techniques with snowpack modeling has allowed for better distributed hydrologic forecasting at the regional scale in complex terrain [*Martinec and Rango*, 1981; *Cline et al.*, 1998; *Marks et al.*, 1999; *Molotch et al.*, 2004]. The snow water equivalent (SWE) reconstruction technique, which sums snowmelt at the pixel-scale for the duration of snowcover as observed by a satellite sensor, has seen dramatic improvements over the last 30 years

[*Martinec and Rango*, 1981; *Cline et al.*, 1998; *Molotch and Margulis*, 2008; *Jepsen et al.*, 2012]. Not only does the SWE reconstruction approach allow for the computation of spatially-explicit maximum SWE accumulation, but it can also provide daily estimates of the spatial distribution of snowmelt and energy balance fluxes [*Jepsen et al.*, 2012].

Hydrologic dynamics and biogeochemical processes likely vary greatly at a relatively small-scale (i.e. sub-catchment) because SWE, snowmelt, landscape subunits, and vegetation are distributed heterogeneously across the landscape. The expansion and contraction of areas that are contributing to snowmelt and/or stream nitrate is also variable in time. The dynamic nature of contributing areas in alpine watersheds is perhaps best characterized by the variable source area concept [*Hewlett and Hibbard*, 1967; *Creed and Band*, 1998; *McDonnell*, 2009], and the relationship between variability in contributing areas and stream solute concentrations can be conceptualized in the hot spots-hot moments biogeochemical model [*McClain et al.*, 2003] (see Background for further discussion). Many recent alpine hydrochemical modeling studies have found that it is crucial to characterize snowmelt on a detailed spatial scale for catchments of various landcover type ratios to appropriately estimate and understand hydrochemical processes [*Campbell et al.*, 1995; *Meixner et al.*, 2000; *Sickman et al.*, 2001; *Liu et al.*, 2004; *Molotch et al.*, 2008]. Wolford *et al.* (1996) and Meixner *et al.* (2000) applied the Alpine Hydrochemical Model (AHM) to the Tokapah Basin (CA), Green Lakes Valley (CO), and Andrews Creek (CO) watersheds for 1 to 2 year periods. The AHM uses discharge and maps of snow covered area (SCA) to roughly estimate spatially-distributed snowmelt, and directs this snowmelt along specific modeled flowpaths to the stream. Molotch *et al.* [2008] applied the SWE reconstruction approach within the AHM, finding that the coupled modeling approach could explain 13% more variability in stream nitrate concentrations. This demonstrates the importance of our

understanding of the spatial distribution of snowmelt for our understanding of alpine hydrochemistry. Using a spatially distributed snowmelt model to explain variability in hydrochemical observations may reveal important interactions between or decoupling of hydrologic and biogeochemical processes. Potential increases in nitrate loading to alpine areas from wetfall may occur concurrently with a changing climate, and our ability to assess a catchment's response to these two events is crucial for both watershed and ecosystem management.

Here, I present a multi-year, intra- and inter-basin study to explore the stream nitrate response to spatially-distributed snowmelt in alpine catchments. Two alpine watersheds differing in their landcover distribution serve as study sites for stream nitrate concentrations over a 12-year period (1996-2007). The Green Lakes 4 Valley, CO has considerable amounts of fractured bedrock and soils and groundwater is a significant contributor to streamflow; the Tokapah Basin, CA has more exposed bedrock and its streamflow has exhibited significant sensitivity to spatially-distributed snowmelt from a SWE-reconstruction model [*Jepsen et al.*, 2012]. If a basin is hydrochemically sensitive to changes in snowmelt and snow accumulation, then the SWE-reconstruction model should have high explanatory power of the variability in stream nitrate. By examining this multi-year record of stream and snowpack chemistry with a spatially distributed snowmelt model, I aim to answer the following questions:

1. Can the SWE reconstruction model be used to explain any of the variability in the concentrations of stream nitrate observed in GLV4 or TOK?
2. Is there a relationship between the rate of nitrate export and the amount of nitrate exported from GLV4 or TOK?

3. What is the magnitude of nitrate-loading to the snowpack and nitrate-export from GLV4 and TOK, and how does this vary interannually?

2. BACKGROUND

This section provides detailed background information on the nitrogen cycle, snowpack-nitrate processes, the variable source area concept, and snowmelt modeling.

2.1 The Nitrogen cycle

Nitrogen can enter alpine environments primarily via atmospheric deposition or biologic fixation [*Butcher et al.*, 1992; *Wetzel*, 1983]. Inorganic forms of N (NO_3^-, NH_4^+) can adsorb to inorganic particulate matter in the atmosphere, and organic N compounds can be found as atmospheric particulates [*Wetzel*, 1983]. Wet deposition occurs when forms of N in the atmosphere are incorporated into and fall to the earth surface via precipitation. Dry deposition of N occurs when particulate solutes are carried from lower to upper-elevations via turbulent processes and settle on the terrestrial surface. N-fixation by the terrestrial environment occurs when plants or microbial communities uptake N_2 gas from the atmosphere for biologic processes.

From here I will follow atmospherically-deposited nitrate (NO_3^-) through the N-cycle. Upon entering the terrestrial environment, atmospherically-deposited nitrate can take several paths. It could undergo denitrification, a microbially-induced reduction reaction, to be released back to the atmosphere as N_2 gas [*Butcher et al.*, 1992]. Plants or microbial communities could fix this N_2 gas to ammonium (NH_4^+) in the soil, where it could undergo nitrification (a series of oxidation reactions) to become nitrite (NO_2^-) and then nitrate again [*Butcher et al.*, 1992]. Atmospherically-deposited nitrate could rather be assimilated by plants, where it would undergo

a series of reactions to become amino acids that can be used for growth [*Butcher et al.*, 1992]. N is an essential element for life, and thus all organic material has N in it. Microbial communities can convert organic N in decaying material to ammonium, which can then undergo nitrification to become nitrite (NO_2^-) and then finally nitrate again [*Butcher et al.*, 1992]. Atmospherically-deposited nitrate could instead be leached from the terrestrial environment into aquatic ecosystems, where it could be transported downstream and/or assimilated by plants in the aquatic environment [*Butcher et al.*, 1992; *Wetzel*, 1983].

2.2 Snowpack-nitrate processes

The seasonal snowpack accumulates with the deposition of frozen precipitation. NO_3- can be deposited from the atmosphere to the terrestrial environment via wet or dry deposition. Solutes that are present in snowfall will accumulate in the snowpack during the winter months, and will only travel through the terrestrial environment when snowmelt begins. Within the snowpack, coupled temperature and pressure gradients induce snow grain metamorphism. As the snow grains undergo metamorphosis, their surfaces accumulate solutes over time. Destructive metamorphism, where snow grains lose mass, results in an accumulation of solutes on the outside of snow grains. Grain surfaces that gain mass experience an accumulation of solutes as well, since the solutes are not well-incorporated into the crystal lattice structure of ice [*Harrington and Bales*, 1998]. Because impurities are at the snow surface and along grain boundaries when snowmelt begins, they are readily flushed from the snowpack with the first melt, known as the "ionic pulse" [*Johannessen and Henriksen*, 1978; *Bales et al.*, 1989]. More than 80% of the solutes can be flushed from the snowpack in the first 20% of snowmelt.

Melt-freeze cycles in the snowpack can enhance the magnitude of solutes released in the first flush, such that the ionic pulse is stronger for snowpacks that experience more melt-freeze events [*Tsiouris et al.*, 1985]. This can result in a magnification of any damaging concentration pulse of pollutants above the snowpack average. Rain events or pulses (i.e. hours) of melt during the winter accumulation months result in smaller earlier pulses of solutes from the snowpack, reducing the strength of the ionic pulse [*Williams et al.*, 1996b; *Sickman et al.*, 2001].

2.3 "Hot Spots- Hot Moments" applied to alpine environments: A geographic biogeochemical model for nitrate

McClain *et al.* [2003] makes a broad argument that effective natural resource management necessitates the prediction of location and timing of processes, such as elemental or hydrologic cycling, within a landscape. The coupling of biogeochemical and hydrologic processes are tightly integrated as water mobilizes solutes and provides conditions for increasing biogeochemical cycling rates [*McClain et al.*, 2003]. McClain *et al.* [2003] partitions the spatiotemporal distribution of accelerated biogeochemical processes into two categories: Hot Spots and Hot Moments, which are broadly defined as relatively small areas and short periods of accelerated biogeochemical processes. Hot Spots often occur at the intersection of hydrologic/substrate flowpaths. Hot Moments often occur during the episodic mobilization of accumulated substrates along hydrologic flowpaths.

The onset of snowmelt can be conceptualized as a Hot Moment of nitrate mobilization from the snowpack and soil to the stream. Nitrate is flushed from the snowpack by meltwater during the ionic pulse. If the melting snowpack is located near a stream, this ionic pulse will likely reach the stream. If a melting snowpack is on or near soil that is adjacent to a stream,

nitrate may be leached from the soil as well, resulting in a Hot Moment of nitrate flushing to the stream. Alternatively, meltwater may induce biological activity, thereby reducing N-leaching to the stream. Scaling nitrate-snowmelt dynamics from a point to a hillslope to the basin scale immediately complicates the Hot Moment model. Hot Moments of nitrate flushing from the snowpack and the soil may or may not result in a Hot Moment of nitrate leaching into the stream, depending on the hydrologic flowpath. A hydrologic flowpath is the path that water takes from the snowpack to the stream through or over landcover subunits such as soil, talus, exposed bedrock, lakes, etc. The hot moment nitrate pulse in an alpine catchment stream at any particular time is highly dependent on the location and timing of snowmelt.

2.4. The Variable Source Area concept: Applications to nitrate and snowpack processes in alpine environments

Variable source area (VSA) hydrology accounts for the spatial distribution of saturated areas that are contributing to runoff [*McDonnell*, 2009]. Hewlett and Hibbard (1967) developed the VSA concept when they observed a stream response to rainfall but saw no overland flow. They hypothesized that this was due to much of the rainfall infiltrating and moving to the stream via shallow sub-surface flow (saturated throughflow). Overland flow only occurred when rainfall occurred on areas that were already saturated (referred to as saturation overland flow, SOF). Areas of saturation expand and contract with varying intensities and amounts of rainfall. The greater the saturated area, the greater the hydrologic connectivity of the basin.

The VSA concept can be expanded to seasonally snow-covered alpine catchments, where source areas of water (i.e. snowmelt) vary in time and space, such that the catchment will experience an expansion and contraction of saturated contributing areas with the onset,

continuation, and decline in snowmelt area. The VSA concept has also been expanded to biogeochemical processes. For example, Creed and Band [1998] used the VSA concept to explain nitrate flushing to the stream in a catchment in central Ontario, finding that the rate of nitrate flushing was proportional to the rate of SOF generated by snowmelt. The soil acted as a sink for nitrate while saturated throughflow was deep below the soil surface, but when the water table approached the soil surface, nitrate was flushed from the soil to the stream [*Creed and Band*, 1998]. The VSA concept applications to snowmelt and to nitrate-flushing can be merged to help explain stream nitrate concentrations during snowmelt. Catchments with deeper, developed soils and greater groundwater capacity may better mitigate stream nitrate loading resulting from atmospheric deposition to the snowpack compared to catchments with more exposed bedrock and shallower flowpaths. This hypothesis may not hold if basins are already nitrate-saturated (i.e. nitrate source exceeds nitrate biological demand).

In the context of stream nitrate dynamics during snowmelt, contributing areas are not defined by the contributing *snowmelt* areas, but rather the contributing *nitrate* areas. In theory, a contributing nitrate area is an area that is experiencing a net flushing of nitrate. This nitrate could be from the snowpack's ionic pulse, soil nitrate flushing, or both. In areas where the snowpack is located above or near soils or talus, the hot moment of nitrate flushing may not occur until enough snowmelt has occurred to effectively saturate the subsurface so that soil nitrate is flushed via shallow saturated throughflow. This would effectively result in a large difference in the timing of initial snowmelt and the stream nitrate pulse. In areas where the snowpack is located above or near exposed bedrock or shallow poorly-developed soils, the hot moment of nitrate flushing may be more concurrent with the timing of initial snowmelt due to shorter more direct flowpaths between the snowpack and the stream.

3. SITE DESCRIPTIONS

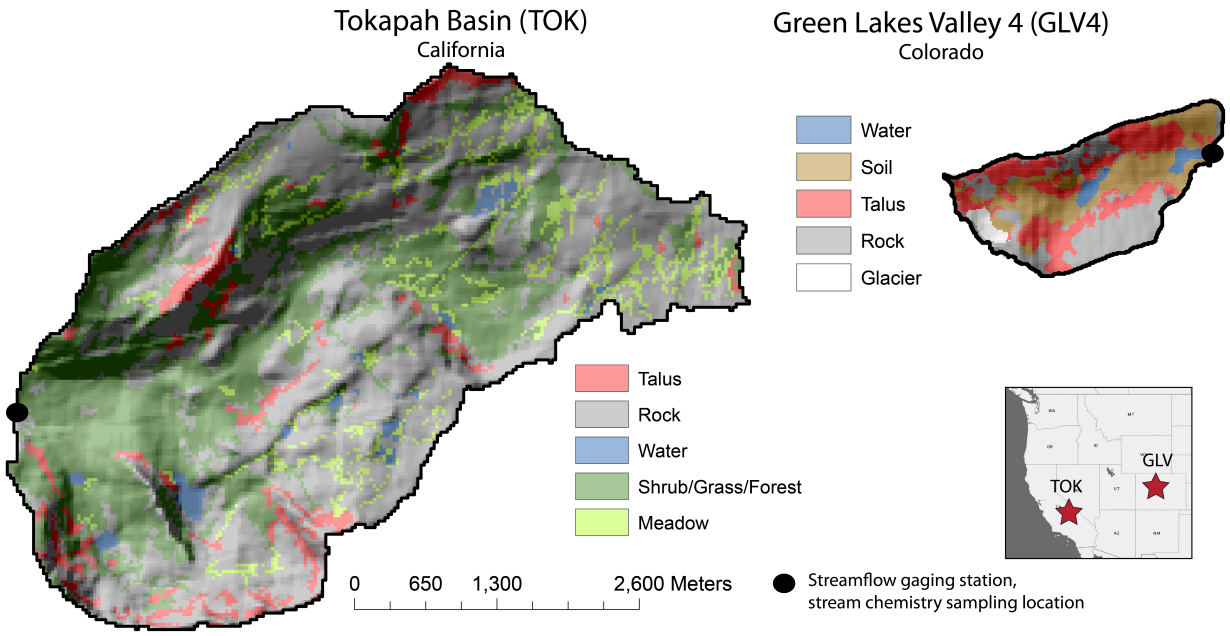

Figure 1. Landcover maps and locations of Tokapah Basin, CA and Green Lakes Valley 4, CO (USA). The locations of discharge and stream chemistry measurements are also displayed (black circle).

3.1 Green Lakes 4 Valley, CO

Green Lakes 4 Valley (henceforth GLV4) (40˚03'N, 105˚35'W) is an east-facing alpine catchment located in the Colorado Front Range, approximately 60 km from the Denver metropolitan area (Figure 1). The 2.2 km^2 GLV4 is situated within the greater 7 km^2 Green Lakes Valley (GLV), which contains a series of five high elevation lakes. The GLV4 catchment encompasses only the upper two lakes (Green Lake 4 and Green Lake 5), and is generally representative of alpine areas in this region. GLV4 stream discharge and chemistry samples were collected at the outflow of Green Lake 4. GLV4 has elevations ranging between 3550 to over 4000 m, and an average slope of 28º [*Jepsen et al.*, 2012]. Approximately 29% of GLV4 is comprised of exposed bedrock [*Erickson et al.*, 2005], which is located on the ridge tops. Soils

(29% of basin area) are located adjacent to the stream channel, and are sparsely vegetated [*Meixner et al.*, 2000; *Erickson et al.*, 2005]. Areas of talus account for 33% of the basin area [*Erickson et al.*, 2005] and are located on the steep slopes between the exposed bedrock and soils. GLV4 also has a glacier at its head. A rock glacier adjacent to Green Lake 5 contains small patches of alpine tundra on its surface [*Williams et al.*, 2006] and has a high concentration nitrate signature in its outflow [*Williams et al.*, 2007].

GLV4 is characterized by a continental climate regime, receiving approximately 80% of its precipitation as snow [*Williams et al.*, 1996b]. Snowmelt typically begins in early to mid-May [*Erickson et al.*, 2005], and as much as 50% of snowmelt may be accounted for by turbulent fluxes (sensible and latent heat) [*Jepsen et al.*, 2012]. Mean annual temperature recorded at a climate station located on Niwot Ridge is -3.7 ºC [*Williams et al.*, 1996b]. Niwot Ridge borders the north boundary of the catchment and is the site for numerous hydrometric and biogeochemical measurements and studies. GLV4 is located within the Niwot Ridge Long Term Ecological Research (LTER) site and the Boulder Creek watershed, and there is a continuous climate record extending back to the 1950s [*Caine*, 1995]. A co-located National Atmospheric Deposition Program collector at the Niwot Ridge Saddle site also provides a continuous record of precipitation and atmospheric deposition of solutes dating back to the early 1980s.

3.2 Tokapah Basin, CA

The Tokapah Basin (henceforth TOK) is an alpine basin located on the west side of the Sierra Nevada mountain range in Sequoia National Park, CA (Figure 1). TOK is relatively remote relative to major metropolitan centers (north of Los Angeles and 200 km southeast of San Francisco), but is only 35 km east of the major agricultural center of the San Joaquin Valley. It

serves as the headwaters of the Kaweah River basin. TOK is approximately 19.1 km^2, with an elevation range spanning 2800 m to 3416 m [*Jepsen et al.*, 2012], approximately 20 km west of the Sierra crest [*Tonnessen*, 1991]. The average slope is 17 º [*Jepsen et al.*, 2012], although the slopes surrounding TOK and its sub-catchments (Emerald, Ruby) are quite steep (median angle of 31 º) [*Williams and Melack*, 1991a]. Exposed granitic bedrock comprises approximately half of the basin area (51%) [*Jepsen et al.*, 2012], and is broken by small benches of talus and poorly developed sandy soils [*Williams and Melack*, 1991b]. Talus only comprises 5% of TOK [*Jepsen et al.*, 2012]. Vegetated soils are found at lower elevations, and these areas of meadow, shrubs, grasses, and forest account for 40% of the total basin area. Soils are generally adjacent to stream channels, and are surrounded by the extensive areas of exposed bedrock. The average soil depth is 0.35 m, and saturated hydraulic conductivity ranges from 1×10^{-4} to 1×10^{-5} m/s [*Williams et al.*, 1993]. The basin also contains several small lakes, and stream chemistry and stream discharge measurements were made at the Marble Fork gaging station at the basin outflow.

TOK is influenced by Mediterranean maritime climate dynamics, with most precipitation (75-90%) falling as snow during the winter months[*Tonnessen*, 1991]. Annual precipitation varies from less than 1m to greater than 2 m [*Williams and Melack*, 1991a; *Jepsen et al.*, 2012]. Snowmelt typically begins in early April [*Molotch and Bales*, 2006], and average winter air temperatures range from -4 to 4 ºC from year to year [*Tonnessen*, 1991].

4. METHODS

To explore the role of VSA hydrology in GLV4 and TOK, correlation analysis between nitrate contributing areas and stream nitrate concentrations was conducted using a 12 year record of

stream chemistry (March-August) and daily modeled distributed snowmelt at a 30 m spatial resolution. A secondary correlation analysis was performed between nitrate flushing times and variability in export behavior following the approach of a previous VSA-nitrate study [*Creed and Band*, 1998]. A nitrate balance was also conducted to explore interannual variability in nitrate loading and export from both basins, and to relate the potential influence of hydrologic dynamics (such as VSA) or SWE accumulation on basin N-export or retention. The observational record and these three analyses are described in further detail below.

4.1 Observations of snowpack and stream chemistry, SWE, and stream discharge

4.1.1 GLV4. Annual snow surveys were timed to the approximate date of peak SWE in GLV4 (generally early May). During snow surveys, snow pits were dug at six locations within the basin. Snow density measurements were made at 10 cm vertical increments using a 1000 cm^3 stainless steel density cutter. Snow depth and density were used to compute total SWE at each snowpit location:

$$SWE = \frac{\rho_{snow}}{\rho_{water}} \times d_{snow} \quad [1]$$

where *SWE* is the snow water equivalent (m), ρ_{snow} is the snowpack density (kg m^{-3}), ρ_{water} is the density of liquid water (1000 kg m^{-3}), and d_{snow} is the snowpack depth (m). Snow samples were also collected in the snowpits for snow chemistry measurements: a sterile PVC tube 50 cm in length was driven vertically in the snowpack, and each 50 cm sample for the entire snowpack was placed in a sealed bag. The resulting final sample was representative of an entire snowpack column. The bottom 10-15 cm of the snowpack was not collected to avoid soil contamination of snowpack chemistry. For some years, these depth integrated snow samples were collected twice

for each pit. These depth-integrated snow samples were later processed in the Kiowa Lab for solute concentrations, including nitrate.

Stream chemistry samples were collected once per month during winter months, and then approximately once per week from May through the summer months. These samples were also processed for a suite of chemical constituents, including nitrate. Because of irregular sampling, the data was linearly interpolated to approximate daily stream nitrate concentrations. Continuous stream discharge estimates were made from daily stage height observations at the GLV4 outflow from May-October. This record extends back to 1982 [*Caine and Thurman*, 1990].

4.1.2 TOK. As in GLV4, annual snow surveys in the TOK were timed to capture a snapshot of the basin at peak SWE (i.e. at the start of the snowmelt season). Snowpit data (density, depth, snow chemistry samples) were collected using similar methods to those described for GLV4. Both SWE and snow chemistry data were available 1996-1999, 2005, and 2007. Density and snow depth measurements were also made throughout the basin using snow depth probes and a Federal Sampler.

Stream chemistry samples were collected daily using an ISCO sampler during the snowmelt season at Marble Fork (the outflow for TOK) for 1996-1999. Samples may have been stored in the ISCO sampler for up to 10 days. A storage effect study was conducted, showing only a slight depression in pH but no significant impact on other solutes in the short-term (personal communication with Jim Sickman, 2012). During 2000 and 2002-2007, samples were collected several times per week or month during the snowmelt season. As for GLV4, data were linearly interpolated to approximate daily stream nitrate concentrations. Stream chemistry

measurements were not available for 2001. Hourly stream discharge measurements were made at the Marble Fork gaging station, and were integrated to daily discharge estimates.

4.2 Stream nitrate response to spatially distributed snowmelt: A new approach to VSA dynamics analysis

To evaluate how the stream nitrate responds to snowmelt, I regressed the daily stream nitrate concentration at the basin outflow against the daily contributing nitrate source area (i.e. areas of nitrate "flushing") for each year. The spatiotemporal distribution of this nitrate contributing area (NCA) was derived from a snow water equivalent reconstruction model product [*Jepsen et al.*, 2012], and describes and quantifies the expansion and contraction of contributing areas. If the variability in NCA explains a significant amount of the variability in stream nitrate concentrations, then it is likely that VSA dynamics describe the catchment's hydrology.

The snow water equivalent reconstruction model and the characterization of contributing areas of nitrate are described in detail below.

4.2.1 Snow water equivalent reconstruction model. Maximum SWE for each grid cell can be reconstructed using the known dates of snow disappearance and maximum SWE, and summing the snowmelt increments between those two dates. The date of maximum SWE is estimated from the dates of snow surveys, which are timed to occur near or at maximum accumulation. Grids of fractional snow-covered area were estimated from Landsat 5 and 7 imagery, using the Thematic Mapper Snow Covered Area and Grain Size algorithm (TMSCAG) [*Painter et al.*, 2009]. Details on correction for canopy and cloud cover are provided in Jepsen *et al.* [2012].

Maximum SWE (SWE_0) is derived from the integration of all of the snowmelt that occurred between the dates of snow disappearance and maximum SWE, such that:

$$SWE_0 = \sum_{j=1}^{n} M_j \quad [2]$$

where M_j is the snowmelt that occurs at time step j, and n is the number of time steps that occur between the dates of maximum SWE and snow disappearance.[1] M_j is approximated from

$$M_j = M_{p,j} SCA_j \quad [3]$$

where $M_{p,j}$ is an increment in potential snowmelt at time step j assuming that 100% of the grid cell is snow-covered, and SCA_j is the fractional snow-covered area of the grid cell at time step j [*Molotch*, 2009; *Jepsen et al.*, 2012]. $M_{p,j}$ is derived from

$$M_{p,j} = E_{p,j}(\rho_w L_f)^{-1} t_{sph} \quad [4a]$$

$$\text{and } E_{p,j} = \max\left[0, min\left[\left(\sum_{k=0}^{j} Q_{net,k}\right), Q_{net,j}\right]\right] \quad [4b]$$

where $E_{p,j}$ is the energy available for snowmelt with respect to the cold content of the snowpack, ρ_w is the density of liquid water, L_f is the latent heat of fusion ($3.34\times10^5\ J\ kg^{-1}$), t_{sph} is 3600 seconds per hour, and $Q_{net,jk,}$ is the net energy flux (W m^{-2}) to the snow surface during time step k or j. $Q_{net,j}$ was calculated by

$$Q_{net,j} = (1 - \alpha_{snow})K_j + L_j + Q_{H,j} + Q_{L,j} \quad [4c]$$

where $\alpha_{snow}$is the albedo of snow, K_j is incident shortwave radiation, L_j is net longwave radiation, $Q_{H,j}$ is the sensible heat flux, and $Q_{L,j}$ is the latent heat flux. The ground heat flux is disregarded, as it is considered an insignificant contributor to the energy flux to the snowpack during the snowmelt season [*Marks et al.*, 1992]. For a detailed description of the calculation of the cold content and calculation of the net energy flux parameters, refer to Jepsen *et al.*, 2012.

[1] New snowfall is not considered in the SWE reconstruction model, as precipitation is considered insignificant after the date of maximum accumulation.

4.2.2. Defining nitrate contributing area. Locations within a watershed have the potential to contribute to the stream nitrate pulse if they are "flushing" nitrate from the snowpack and/or the soil. Henceforth, we refer to the sum of these locations within a catchment as the nitrate contributing area (NCA, fraction of total basin area). After a pixel has "flushed," it may still be contributing hydrologically but has theoretically finished contributing nitrate, and is presumably only contributing to solute dilution in the stream. I have developed a conceptual approach for characterizing NCA three different ways: (A) areas are contributing if they have melted above a given threshold (cm day^{-1}) for less than a particular number of days, (B) areas are contributing until they have lost the threshold fraction of their maximum SWE, and (C) areas are contributing until a threshold amount of SWE has melted. These definitions are detailed below, and in Table 1. "Melting" areas were defined as locations of SWE loss greater than 5 mm day^{-1}, and a fractional snowmelt area (FSMA) of the basin was computed as the snowmelt area as a fraction of the total basin area.

NCA definition A: Melt duration. For this definition, pixels are contributing if the number of days a pixel has been melting is below a specified threshold number of days. I set three "melt-day" thresholds: 3 days (NCA1), 7 days (NCA2), and 10 days (NCA3). A pixel was considered to be contributing its solutes (from the snowpack and from the subsurface) from the time it first began melting until it exceeded the allowed number of melt-days (i.e. 3, 7, or 10 days).

NCA definition B: Melting up to a percent-loss of SWE. For this definition, pixels are contributing when they melting up until they have lost a certain threshold percent of their maximum SWE. As described above, this is related to the ionic pulse concept [*Johannessen and Henriksen*, 1978]. I set these percent-mass thresholds at 20% (NCA4),

35% (NCA5), and 50% (NCA6). Note that this definition results in variability in the absolute amount of melt required to flush a pixel, as the percent loss is a function of the maximum SWE per pixel, which varies spatially.

NCA definition C: Melting up to an absolute-melt. For this definition, pixels are contributing when they are melting up until an absolute threshold in depth of melt has occurred. These absolute-depth thresholds were set at 10 cm (NCA7), 20 cm (NCA8), and 30 cm (NCA9) of snowmelt.

Table 1. Nitrate Contributing Area (NCA) definitions

Definition	Characterization of flushing snowpack (per pixel)
NCA1	Pixel has been melting for up to 3 days
NCA2	Pixel has been melting for up to 7 days
NCA3	Pixel has been melting for up to 10 days
NCA4	Pixel SWE ≤ 20% melt-loss of initial maximum SWE
NCA5	Pixel SWE ≤ 35% melt-loss of initial maximum SWE
NCA6	Pixel SWE ≤ 50% melt-loss of initial maximum SWE
NCA7	Pixel SWE ≤ initial maximum SWE−10 cm SWE
NCA8	Pixel SWE ≤ initial maximum SWE−20 cm SWE
NCA9	Pixel SWE ≤ initial maximum SWE−30 cm SWE

*Note that in order for a pixel to be included in the NCA, it must be actively melting. Pixels were not counted as NCA for a particular day if they were not experiencing melt.

4.3 Nitrate export behavior: A secondary approach to VSA dynamics analysis

Creed and Band [1998] used a multi-basin comparison study to determine basins that exhibited VSA behavior in their nitrate flushing. To do this, they regressed monthly cumulative DIN-export on monthly cumulative discharge. They then computed the catchment-specific export residuals by comparing the catchment's DIN export-discharge relationship to the average DIN export-discharge relationship for all of the basins in the study. Next, they computed the average time constant, which is the amount of time for the peak nitrate to be reduced 63%. Finally, they

regressed the catchment-specific average export residuals on the catchment-specific average time constants. They hypothesized that if VSA dynamics regulated the hydrology of a basin, short time constants would be associated with low DIN export and that long time constants would be associated with high DIN export.

I followed a similar methodology to Creed and Band [1998], but instead used a temporal (rather than spatial) approach using the data record from 1996-2007 for each basin (described previously). For each basin, I fitted an exponential decay function to the declining limb of the stream nitrate concentration (μeq L^{-1}) for each year, such that:

$$N(t) = N_{max} e^{-kt} \quad [5]$$

where *N(t)* is the stream nitrate concentration (μeq L^{-1}) at time *t*, N_{max} is the peak stream nitrate concentration (μeq L^{-1}), and *k* is the decay coefficient (day^{-1}). I then computed the annual time constants (T_c) by:

$$T_c = \frac{1}{k} \quad [6]$$

where T_c is number of days it takes for the stream nitrate concentration to be reduced to 37% of its peak value. An example of this is shown in Figure 2A. Second, I regressed cumulative seasonal DIN export (kg-N ha^{-1}) on cumulative seasonal discharge (mm), and computed the annual export coefficient residuals (year-specific export behavior minus average catchment export behavior for the 12 year record) (example in Figure 2B).

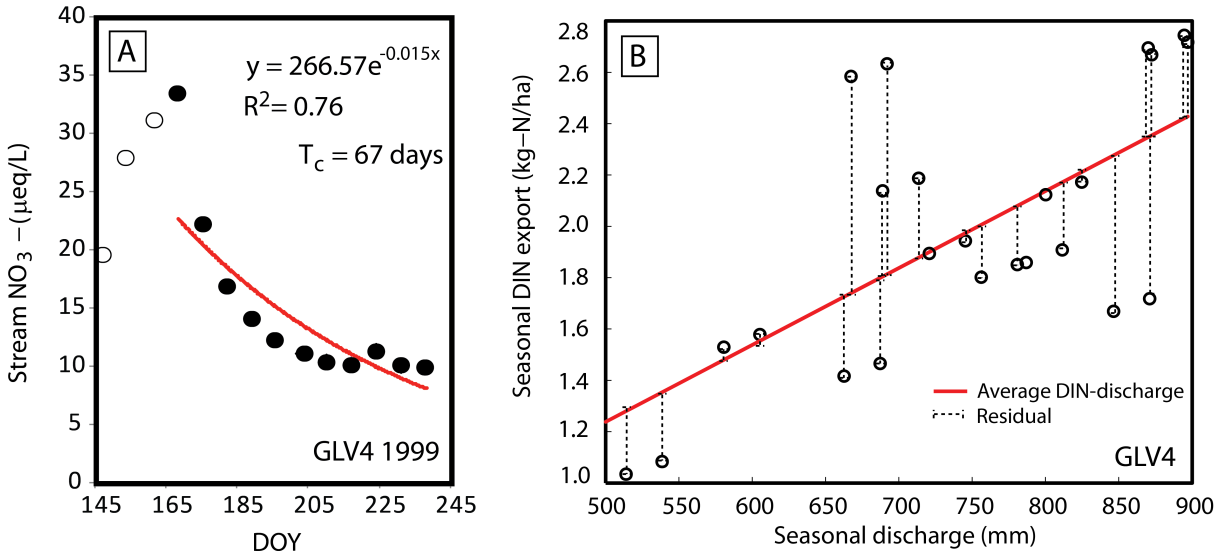

Figure 2. (A) Example of computing the time constant of nitrate flushing (GLV4 1999 shown). The red line is the fitted exponential decay function. Open circles are data points that were not included in fitting the exponential decay function, as they occur prior to the peak stream nitrate concentration. (B) Example of computing the DIN-discharge residuals (GLV4 is shown). The red line is the average catchment DIN-discharge behavior and the dotted lines are the annual residuals.

Finally, I regressed the seasonal export coefficient residuals on the time constants for TOK and GLV for each year. If the catchment exhibited low DIN-export in years with short time constants and high DIN-export in years with long time constants (i.e. positive correlation between DIN-export and time constants), then VSA dynamics may apply.

4.4 Nitrate mass balance

To conduct a nitrate balance, I compared the mass of nitrate in the snowpack at maximum accumulation with the mass of nitrate that exits the basin via stream flow. In theory, if all sources of nitrate to the stream were from atmospheric deposition to the snowpack, or the amount of nitrate biologically assimilated from snowmelt water was equal to the amount of biologically-produced nitrate flushed from the soil by snowmelt, then

$$maximum({NO_3}^-_{\text{snow}}) = \sum_{j=1}^{n} {NO_3}^-_{stream,j} \quad [7]$$

where $maximum({NO_3}^-_{\text{snow}})$ is the total mass of snowpack nitrate (mg), ${NO_3}^-_{stream,j}$ is the mass of nitrate in the stream at any timestep *j*, and *n* is the total number of timesteps from the time of $maximum({NO_3}^-_{\text{snow}})$ to the end of the sampling period. The integration of the stream nitrate over the sampling season was dependent on the date of the snow survey or the initiation of discharge observations for the start-date (whichever occurred later). Date ranges for the seasonal cumulative stream nitrate can be found in the Results section (Table 3).

I assumed that the data collected during the snow surveys were representative of the maximum SWE and total winter nitrate-loading to the snowpack. I first computed the nitrate-load for each sampling site, and then averaged the site-specific nitrate-loading values for the basin. I computed the total mass of snowpack nitrate-loading to the basin by

$$ {NO_3}^-_{\text{snow,mass}} = maximum({NO_3}^-_{snow,conc.}) \times SWE \times A \quad [8] $$

where ${NO_3}^-_{snow,conc.}$ is the concentration of nitrate in the snow (μeq L^{-1}, converted to mg m^{-3}), *SWE* is the snow water equivalent (m), and *A* is the basin area (m^2).

Available stream nitrate data were available as values of concentration (μeq L^{-1}, equivalent to μmol L^{-1}), and were converted to mass of stream nitrate per day by

$$ N_{stream} = Q \times [{NO_3}^-_{stream}] \quad [9] $$

where ${NO_3}^-_{stream}$ is the mass of nitrate in the stream (mg day^{-1}), Q is stream discharge (L day^{-1}), and $[{NO_3}^-_{stream}]$ is the stream nitrate concentration (mg L^{-1}).

5. RESULTS

5.1 Maximum SWE accumulation, and peak stream and snow nitrate concentrations

In general, TOK received more water accumulation in the snowpack than GLV4. Maximum SWE (derived from the SWE reconstruction model) in GLV4 was 60% that of TOK (0.8 m and 1.15 m for GLV4 and TOK, respectively) (Figure 3, upper left panel). The two catchments exhibited similar interannual variability in maximum SWE, with coefficients of variation (CV, the standard deviation as a fraction of the mean) of 0.25 and 0.26 for GLV4 and TOK, respectively. The average nitrate concentration measured in the snowpack at maximum SWE accumulation in GLV4 for all years of measurement was 7.89 $\mu eq\ L^{-1}$, approximately 3.6 times that of TOK (mean value of 2.21 $\mu eq\ L^{1}$) (Figure 3, top right panel). TOK exhibited greater variability in the snowpack nitrate concentration, as the CV for TOK was 0.52, and 0.17 for GLV4. The peak stream nitrate concentration in GLV4 was on average 3.9 times that of TOK (31.06 $\mu eq\ L^{-1}$ and 7.95 $\mu eq\ L^{-1}$ for GLV4 and TOK, respectively). TOK exhibited notably more interannual variability in the peak stream nitrate concentration (Figure 3, bottom right panel), with CVs of 0.63 and 0.18 for TOK and GLV4, respectively. The peak stream nitrate concentration occurred an average of 45 days earlier in TOK than GLV4, and this date was more variable in TOK than GLV4 (standard deviations of 55 days and 10 days for TOK and GLV4, respectively) (Figure 3, bottom left panel).

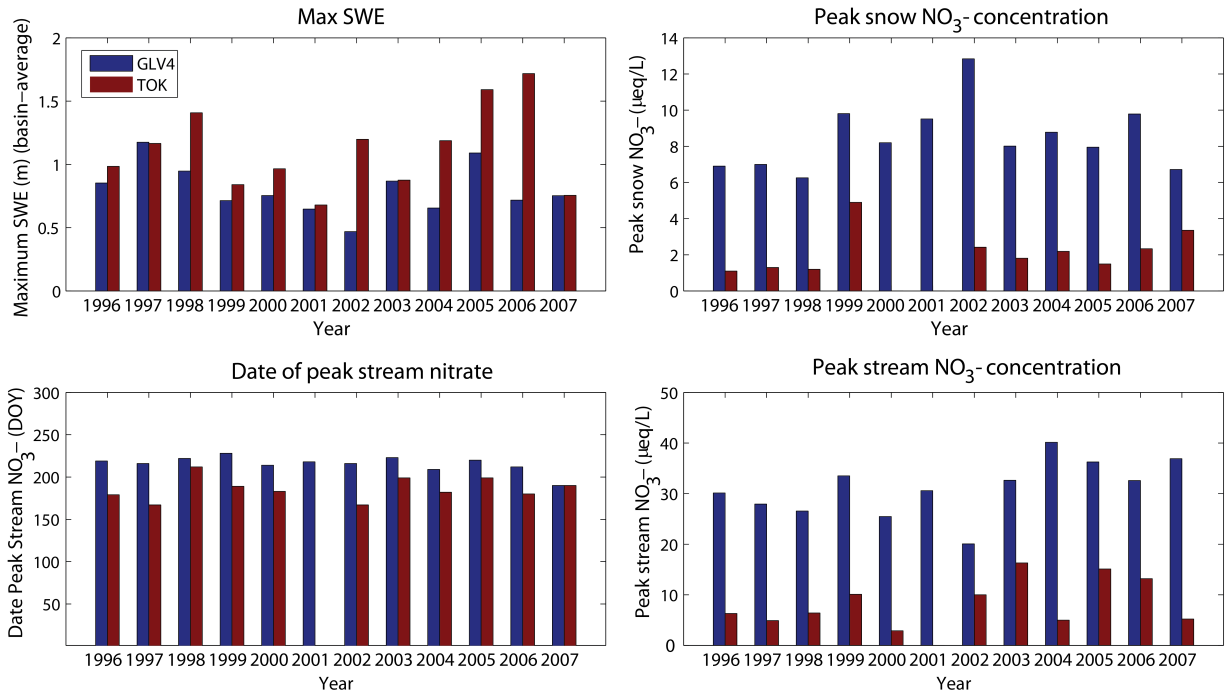

Figure 3. Basin-average maximum SWE values (from SWE reconstruction), peak snow nitrate concentrations, date of peak stream nitrate concentrations, and peak stream nitrate concentrations.

5.2 Stream nitrate response to spatially distributed snowmelt

On average, GLV4 reached a maximum fractional snowmelt area (FSMA) of 0.94 (for 1995-2007). The maximum FSMA was not sustained for more than 1-5 days, and GLV4 experienced intermittent melt periods regularly prior to the dominant extended snowmelt period (oscillating black lines, Figure 4). The falling limb of the stream nitrate concentration was generally concurrent with the falling limb of FSMA. Compared to GLV4, TOK exhibited different patterns of FSMA during the snowmelt period (Figure 5). On average, the maximum FSMA was 0.98 (for 1996-2007) for TOK. Whereas GLV4 experienced numerous intermittent short periods of snowmelt, FSMA in TOK oscillated prior to a long period of sustained high FSMA where almost the entire basin remained melting for longer than a one-week period. After this extended period

of snowmelt, TOK exhibited a rapid decline in FSMA. In general, stream nitrate concentrations declined during the extended period of high FSMA.

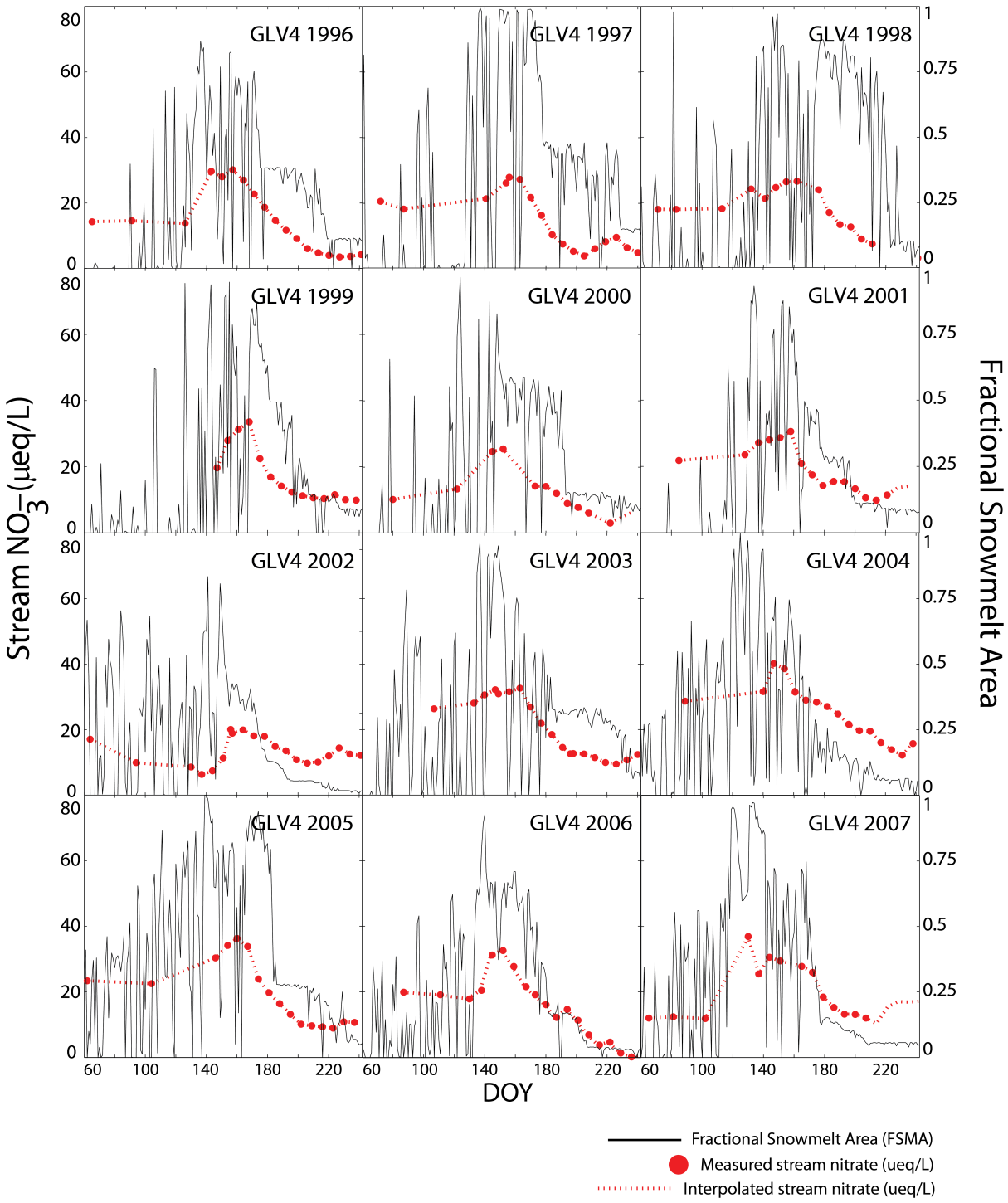

Figure 4. Daily FSMA (black) and outflow NO_3- concentrations (red) for GLV4. Stream chemistry measurements are shown as red circles; these irregular measurements were interpolated to daily values (shown as red dotted line).

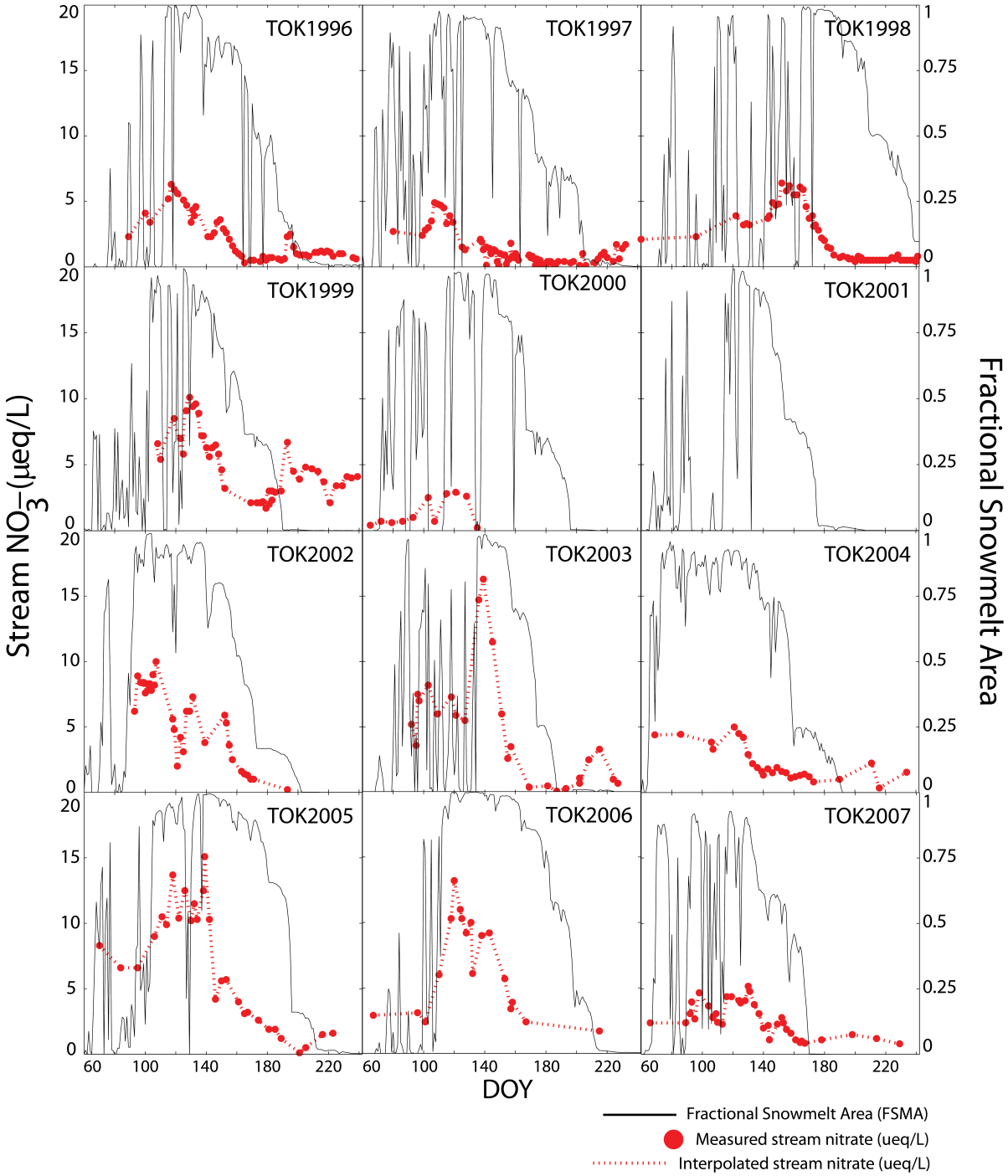

Figure 5. Percent of basin area that is melting (black) daily and the outflow NO_3- concentration (red) for TOK. Stream chemistry measurements are shown as red circles; these irregular measurements were interpolated to daily values (shown as red dotted line). Stream NO_3- data were not available for 2001.

Although FSMA is descriptive of sources of water to the basin outflow, it is not necessarily descriptive of sources of nitrate to the basin outflow. For both basins, nitrate contributing area (NCA, fraction of total basin area) was compared to the stream nitrate concentration for each year using correlation analysis (example shown in Figure 6). All relationships exhibited log-linear relationships between NCA and the stream nitrate concentration.

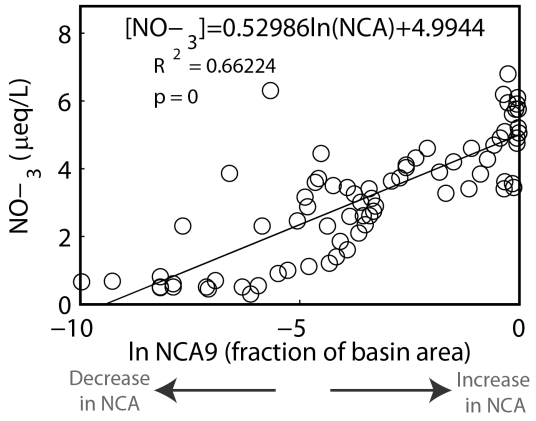

Figure 6. Example of NCA-nitrate correlation plot, where the stream nitrate concentration is compared to the log of the contributing flushing area of the basin. This particular example is for TOK 1996, for NCA9 (30 cm of melt).

Of the best-fit NCA definitions (i.e. statistically significant relationships between different NCA definitions and the stream nitrate concentration), TOK exhibited better correlation between NCA and stream nitrate concentration (mean significant R^2 of 0.68 for best-fit definitions for each year) than GLV4 (mean significant R^2 of 0.44 for best-fit definitions for each year) (Figure 7). On average, the best-fit NCA definition for GLV4 was NCA6 (50% SWE loss). R^2 values using NCA6 in GLV4 ranged from 0.27 to 0.65 and averaged 0.35. On average, the best-fit NCA definition for TOK was NCA9 (30 cm SWE loss). R^2 values using NCA6 in TOK ranged from 0.17 to 0.71 and averaged 0.54. In GLV4, 7 of 12 years exhibited an inverse

relationship between NCA and stream nitrate concentration (1997, 2000, 2002, 2004-2007). In TOK, all 11 years exhibited positive relationships between NCA and stream nitrate concentration (1996-2000, 2002-2007). Positive or inverse relationships were not associated with higher or lower R^2 values.

In GLV4, other models that were best-fit for particular years were NCA2 (1997) (7 days melt), NCA4 (2004, 2005, 2007) (20% SWE loss), and NCA7 (1996, 2000, 2006) (10 cm SWE loss). In TOK, NCA5 (2005) (35% SWE loss), NCA6 (1999) (50% SWE loss), and NCA8 (2000) (20 cm SWE loss) exhibited the highest correlation for their respective years. I did not find a significant relationship between the best-fit NCA definition and maximum basin SWE, date of onset of snowmelt, date of peak stream nitrate, or peak stream nitrate concentration.

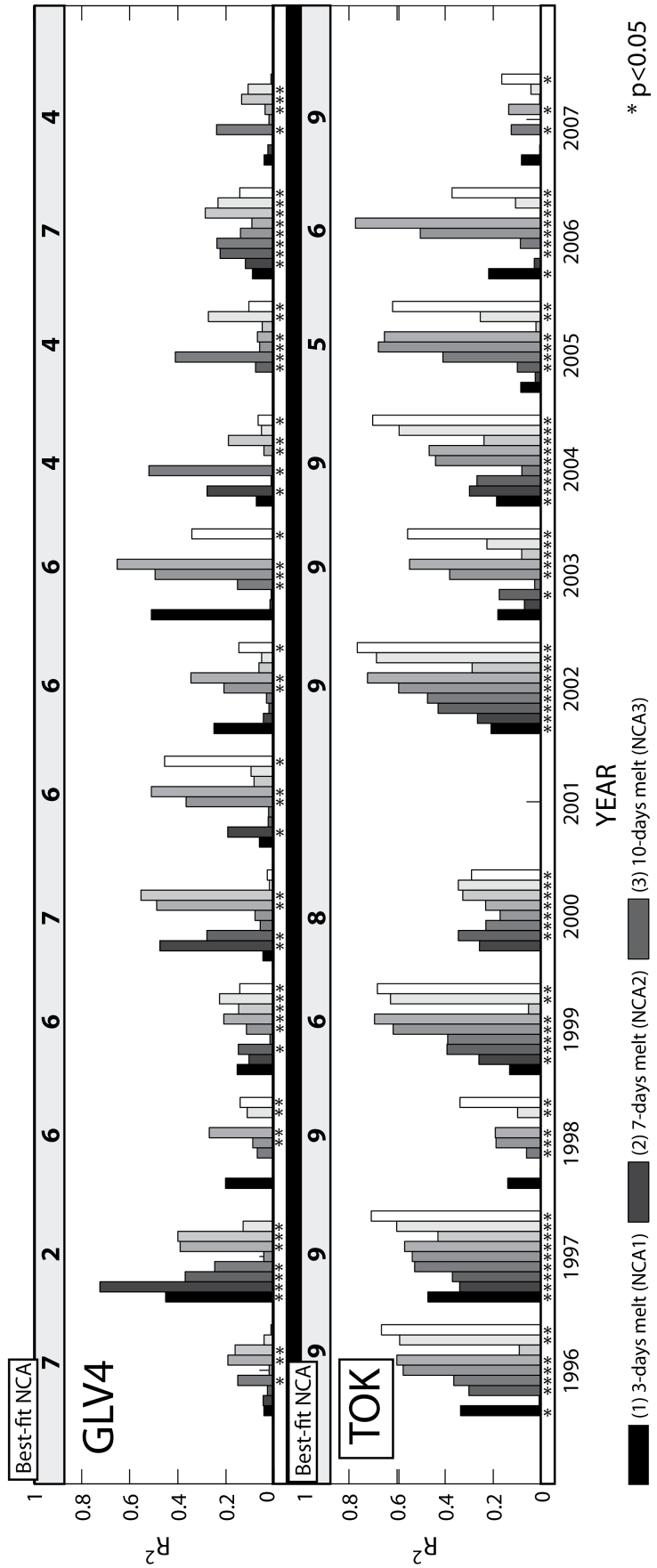

Figure 7. R^2 values for all flushing definitions, for GLV4 and TOK 1996-2007. The definition of best-fit is noted above each year. Significant correlation coefficients ($p<0.05$) are marked with an asterisk.

A pixel was considered "flushed" on the day of year (DOY) it exceeded the NCA threshold (set in the NCA Definitions). As described previously, for GLV4, pixels were considered "flushed" once they had lost 50% of their maximum SWE (NCA6). The spatial distribution of flushing in GLV4 appeared to somewhat be related to areas of wind redeposition (Figure 8); the areas that tend to be wind scoured (upper elevation ridge tops along the northern basin perimeter) were flushed earlier than the lower elevation areas in the valley bottom that are prone to deeper snow depths from wind deposition [*Jepsen et al.*, 2012]. For TOK, pixels were considered flushed once they had lost 30 cm of SWE (NCA9). The spatial distribution of the timing of flushing in TOK appeared to mostly follow an elevational gradient, from low elevation to high elevation areas (Figure 9). It also appeared that aspect may also play a role in the timing of flushing in TOK, with south and west facing slopes generally flushing before north or east facing slopes. From examining average flushing dates for catchment subunits (i.e. landcover types) within each basin (using NCA6 for GLV4 and NCA9 for TOK), GLV4 exhibited generally more spatiotemporal variability in terms of flushing than TOK. Soil was "flushed" 3 days later than talus and 13 days later than rock (i.e. exposed bedrock), and talus was "flushed" 10 days later than rock (Figure 10, upper panel). In TOK, different landcover types were generally "flushed" at the same time (Figure 10, bottom panel).

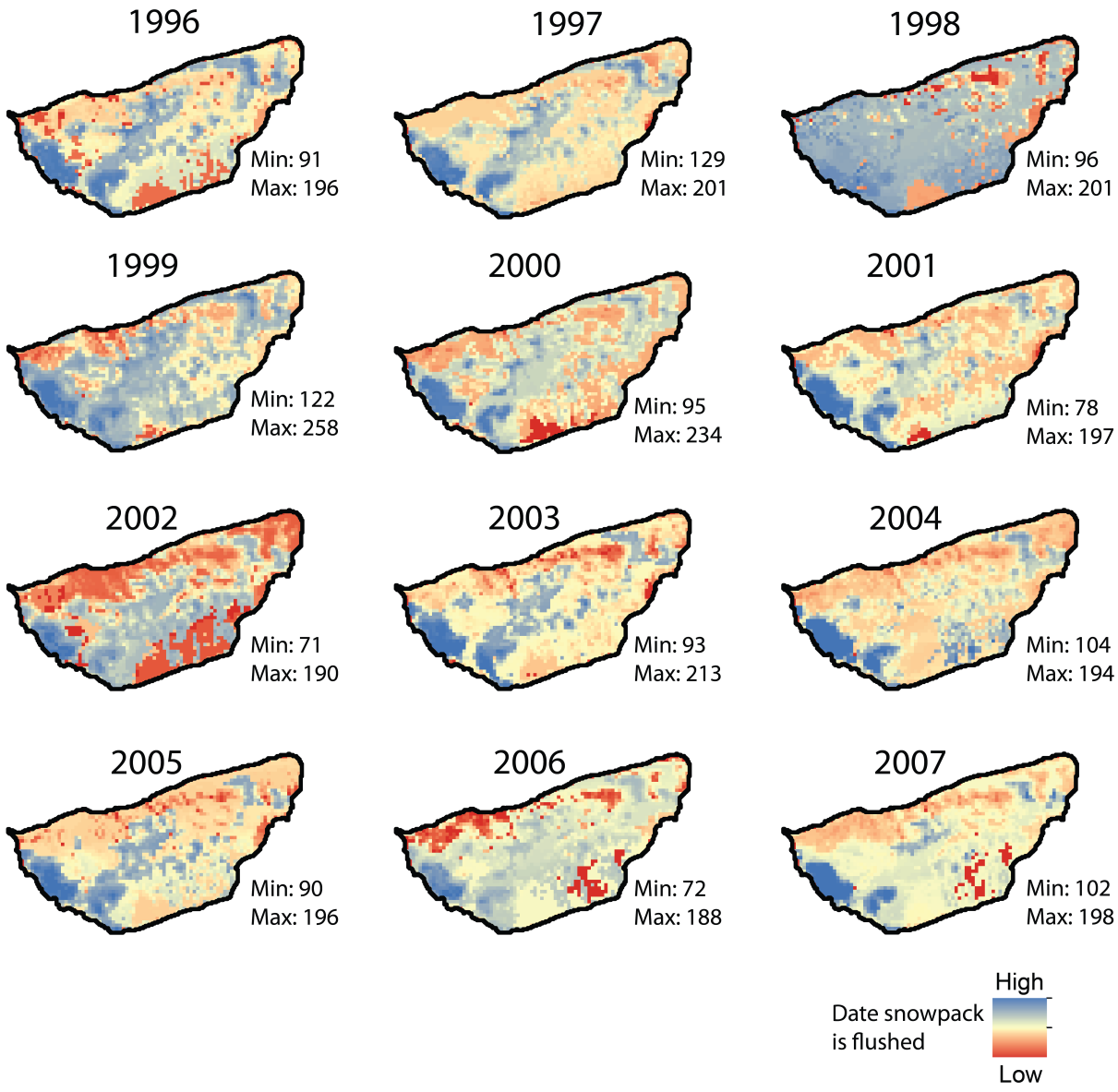

Figure 8. Timing of snowpack flushing in GLV4 for 1996-2007 using NCA6. Red indicates the earliest flushing dates (i.e. min, DOY), and blue indicates the later flushing dates (i.e. max, DOY).

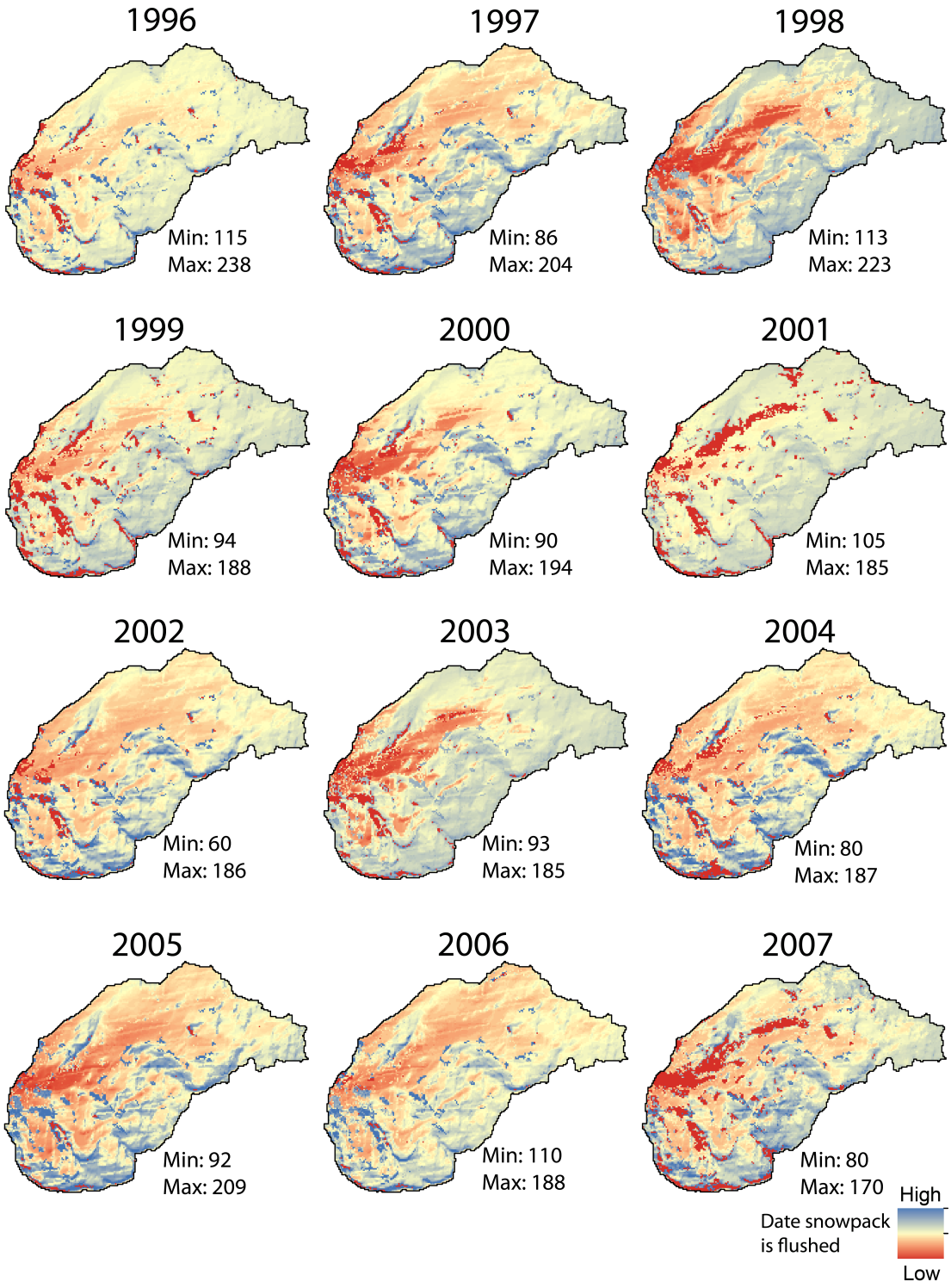

Figure 9. Timing of snowpack flushing in TOK for 1996-2007 using NCA9. Red indicates the earliest flushing dates (i.e. min, DOY), and blue indicates the later flushing dates (i.e. max, DOY).

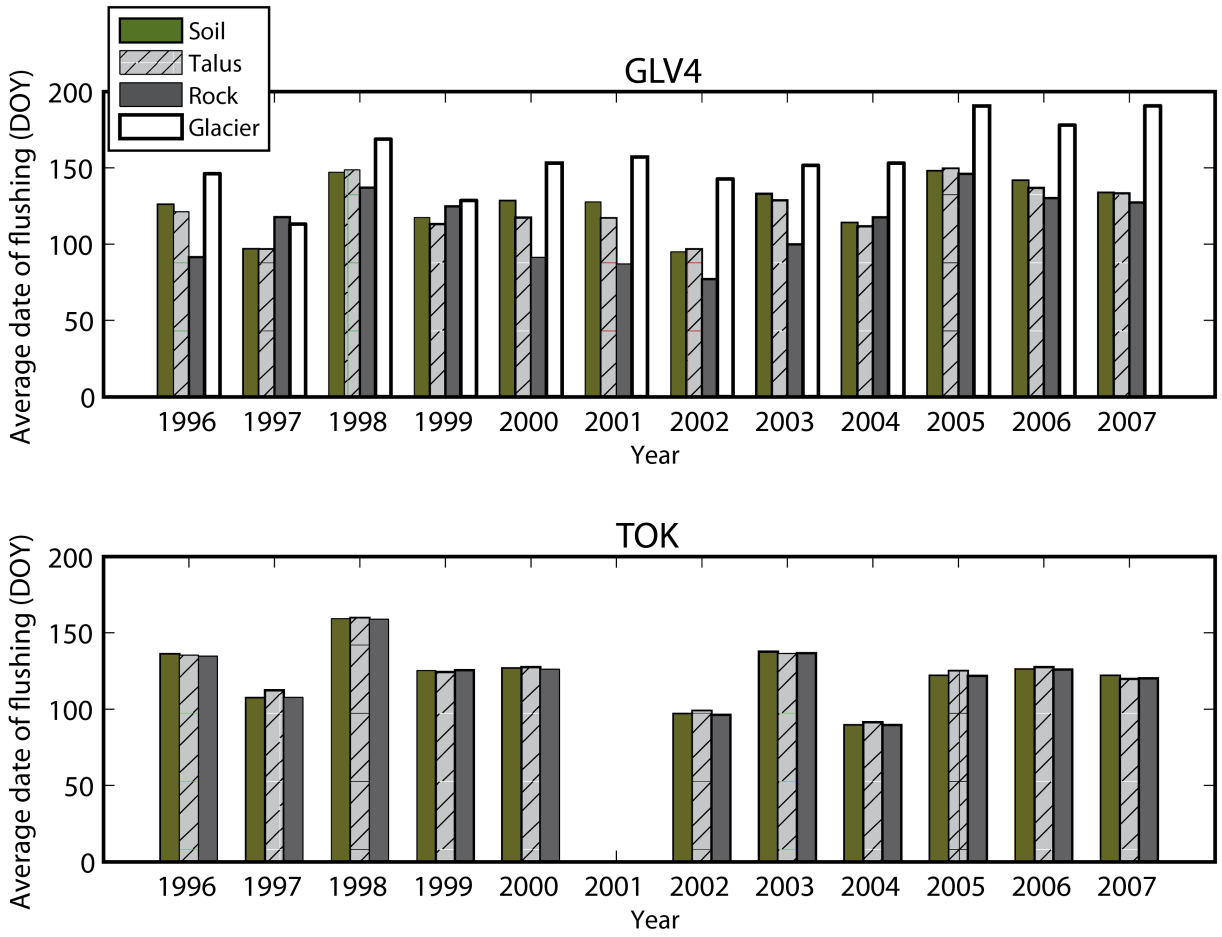

Figure 10. Average date of flushing for basin subunits in GLV4 (upper panel) and TOK (lower panel).

5.3 Nitrate export behavior

The onset of snowmelt timing was computed from the SWE reconstruction product. I derived a time series of the FSMA (fractional snowmelt area) and defined onset of melt date as the DOY when FMSA exceeded 0.20. I did a basic preliminary analysis of hydrochemical lag times with respect to nitrate. On average, GLV4 exhibited a hydrologic lag time (difference between onset of snowmelt and peak stream discharge) of 85 days, which was significantly different than TOK's hydrologic lag time of 60 days (significant at α=0.05) (Figure 11A). I found a nitrate-snowmelt lag time (difference between onset of snowmelt and peak stream nitrate) of 41 days

and 67 days on average for TOK and GLV4, respectively (Figure 11B). TOK was three times more variable than GLV4 with respect to nitrate-snowmelt lag time (CVs of 0.57 and 0.20 for TOK and GLV4, respectively). I found an average nitrate-discharge lag time (difference between peak discharge and peak stream nitrate) of 19 days for TOK, which was significantly different than the 17-day average nitrate-discharge lag time for GLV4 (α=0.05) (Figure 11C). The shortest nitrate-discharge lag time occurred in 1999 for GLV4 (5 days). In 2007 in TOK, peak discharge occurred on the same day as the nitrate pulse. The longest nitrate-discharge (43 days) and shortest nitrate-snowmelt lag times for TOK both occurred in 2002. The longest nitrate-discharge lag time in GLV4 was in 2007 (43 days), which was also a year of lower SWE accumulation, earlier onset of snowmelt (DOY 69), and less spatiotemporal variation in basin flushing (as described previously, see Figure 10). Like the nitrate-snowmelt lag time, the nitrate-discharge lag time was highly variable in TOK; nitrate-discharge lag time varied from the mean by approximately 85% (CV = 0.85; CV for GLV4 = 0.21).

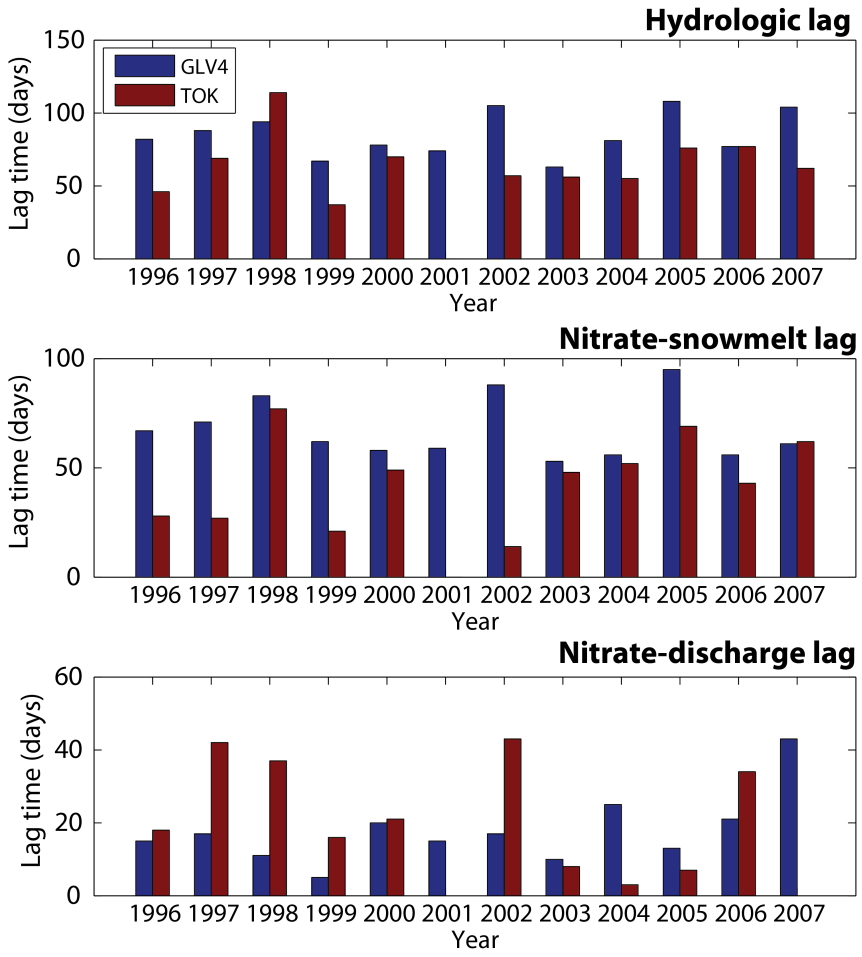

Figure 11. (A) The difference in timing of onset of snowmelt (FSMA>0.2) and peak stream discharge. (B) The difference in timing of the onset of snowmelt (FSMA>0.2) and peak stream NO_3- concentration. (C) The difference in timing of peak stream discharge and peak stream NO_3- concentrations.

I followed the approach of Creed and Band [1998] to analyze the relationship between DIN (nitrate and ammonia) export and flushing time (described previously) (for summary, see Table 2). I found the N-export (N-NO_3-) regression coefficients (slopes of red lines, Figure 12A) to be 3×10^{-3} kg-N ha^{-1} mm^{-1} and 5.3×10^{-4} kg-N ha^{-1} mm^{-1} for GLV4 and TOK, respectively. The average time constants were 69 days and 25 days for GLV4 and TOK, respectively. From a regression of export residuals on flushing time for each year, TOK exhibited a statistically insignificant ($p>0.05$) negative relationship between export residuals and flushing times

(inconsistent with VSA dynamics under this model) (Figure 10B, open circles). GLV4 exhibited a statistically insignificant ($p>0.05$) positive relationship between export and flushing time (also inconsistent with VSA dynamics under this model) (Figure 12B, closed circles).

Table 2. Summary statistics for linear regression of seasonal catchment DIN export and seasonal discharge, and for computation of flushing times from fitting an exponential function to the decline in stream nitrate concentration. Residuals (%) were normalized by dividing the annual residuals by the average catchment behavior (i.e. linear regression for DIN export-seasonal discharge).

	GLV				TOK			
	Regression coefficient = 3.0×10^{-3} kg-N ha^{-1} mm^{-1} $R^2 = 0.41$ ($p<0.05$)				Regression coefficient = 5.3×10^{-4} kg-N ha^{-1} mm^{-1} $R^2 = 0.54$ ($p<0.05$)			
Year	Residual	Residual (%)	k	$T_c = k^{-1}$ (days)	Residual	Residual (%)	k	$T_c = k^{-1}$ (days)
1996	-0.261	-12.062	0.029	34	-0.198	-31.548	0.056	18
1997	-0.631	-26.889	0.05	20	-0.343	-62.979	0.038	26
1998	0.030	1.956	0.028	36	-0.306	-39.982	0.032	31
1999	-0.037	-1.697	0.015	67	0.123	42.437	0.028	36
2000	-0.330	-18.411	0.021	48	N/A	N/A	N/A	N/A
2001	-0.027	-1.387	0.009	111	N/A	N/A	N/A	N/A
2002	-0.264	-19.601	0.007	143	0.12	19.563	0.059	17
2003	0.323	13.359	0.015	67	0.284	58.93	0.124	8
2004	0.823	45.516	0.012	83	-0.074	-23.027	0.032	31
2005	0.289	11.934	0.018	56	0.221	31.935	0.051	20
2006	-0.227	-10.937	0.053	19	0.208	24.944	0.023	43
2007	0.313	16.715	0.007	143	-0.035	-31.127	0.041	24
				Mean T_c = 69 days				Mean T_c = 25 days

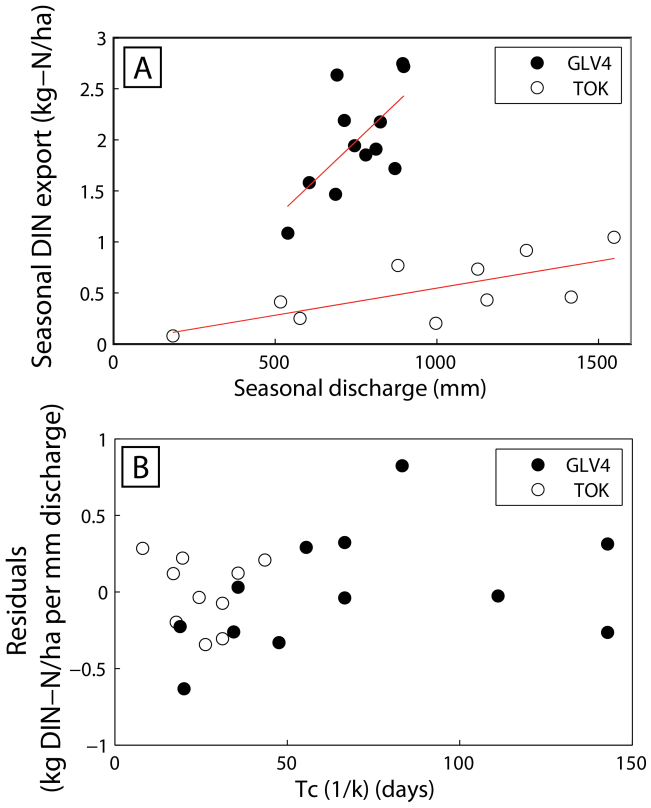

Figure 12. (A) Cumulative seasonal discharge v. cumulative seasonal DIN export. The red lines are the average catchment N-export behavior for each basin. (B) Time constants (Tc) vs. DIN-export residuals.

5.4 Nitrate mass balance

I computed the masses of N in nitrate (N-NO_3-) in the snowpack (N_{snow}) and stream (N_{stream}) during the snowmelt season for each basin (Table 3, Figure 13). N_{snow}-loading was on average 2.8 times greater in GLV4 than TOK (kg-N ha^{-1}, normalized for basin area). N_{stream} leaving the basin over the season (i.e. cumulative seasonal stream N) was on average 4.1 times greater in GLV4 than TOK (kg-N ha^{-1}, normalized for basin area). By subtracting N_{snow} (into the basin) from N_{stream} (out of the basin), I approximated the amount of N retained by the basin (N-retention, a negative value) or the amount of "extra" N (from soil flushing) exported from the basin in the stream outflow (N-export, a positive value). GLV4 exhibited high levels of N-export

for all years except 2002 (Figure 13). TOK exhibited both N-export (1996, 1998, 2002, 2003, 2005, 2006) and N-retention (1997, 1999, 2004, 2007), but export/retention as a percent of the N-loading (N_{snow}) was approximately 38% less than that of GLV4 on average (90% of N_{snow} and 128% of N_{snow} for TOK and GLV, respectively). These results may indicate N-saturation in GLV4.

Table 3. Cumulative masses of N-NO_3- in the snowpack and stream during the snowmelt season.

	Snowpack NO_3- (kg-N/ha)		Cumulative seasonal stream NO_3- (kg-N/ha)		Season length (DOY)	
Year	**GLV4**	**TOK**	**GLV4**	**TOK**	**GLV4**	**TOK**
1996	0.70	0.19	1.80	0.41	days 123-242	days 102-239
1997	0.83	0.22	1.64	0.18	days 154-240	days 99-232
1998	0.78	0.28	1.53	0.41	days 146-240	days 123-241
1999	0.88	0.47	2.08	0.24	days 147-238	days 135-242
2000	0.90	N/A	1.37	0.10	days 131-287	days 66-136
2001	0.99	N/A	1.86	N/A	days 129-235	N/A
2002	1.24	0.41*	1.04	0.73	days 126-241	days 93-193
2003	0.68	0.22*	2.59	0.77	days 123-240	days 92-227
2004	0.89	0.36*	2.48	0.25	days 132-239	days 69-234
2005	0.73	0.34	2.59	0.87	days 131-237	days 92-223
2006	1.16	0.56*	1.79	1.05	days 137-243	days 67-215
2007	0.88	0.31	2.04	0.07	days 128-215	days 92-229

* SWE data to compute N loading was derived from SWE reconstruction product when pit-obervations of SWE were not available. For all other years, snowpit-collected SWE data were used with the corresponding nitrate samples. “Season length” refers to the period of accumulated masses of stream nitrate.

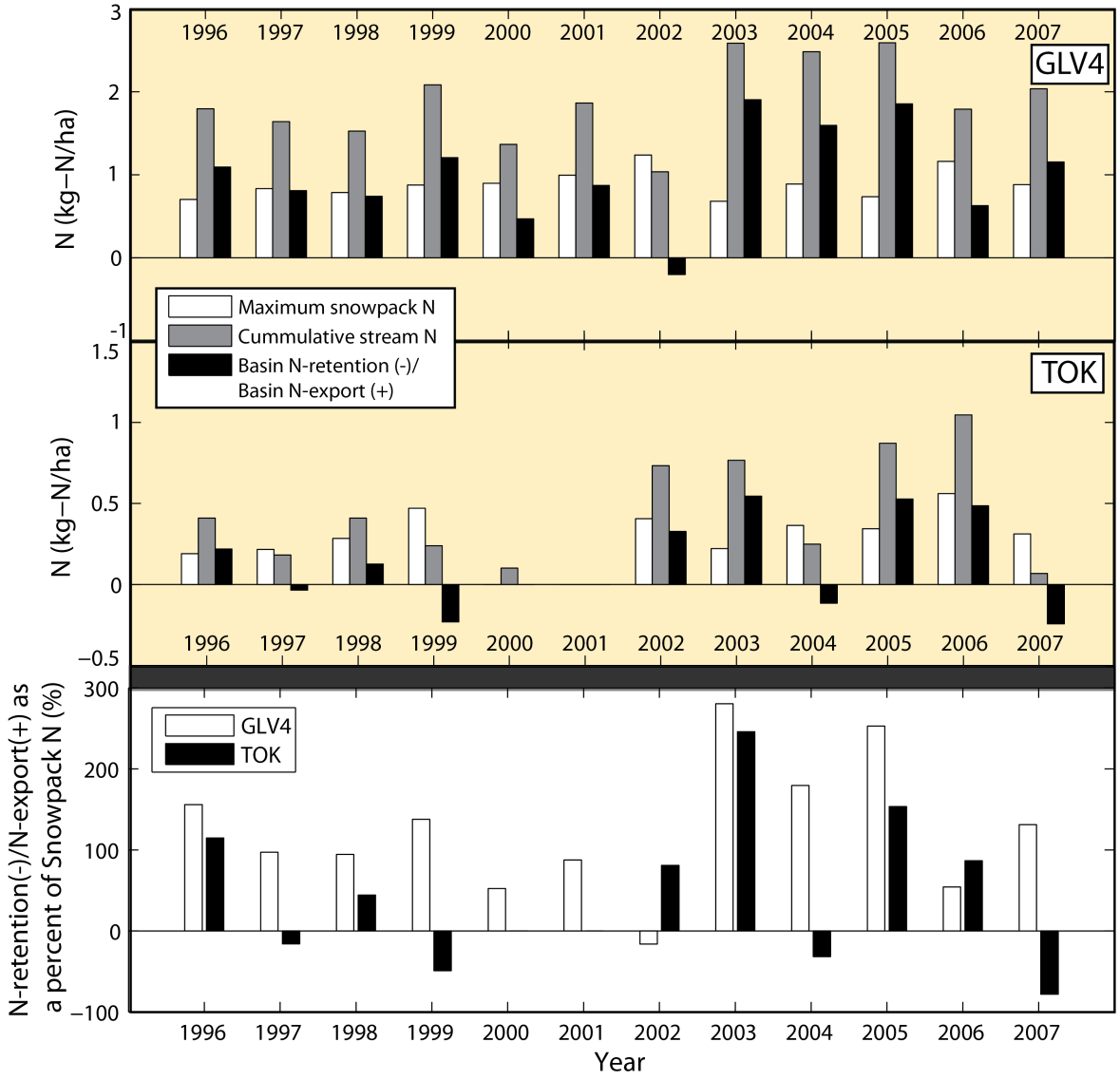

Figure 13. Cumulative masses of N-NO_3- in the snowpack and stream for GLV4 (top panel) and TOK (middle panel). In the top two panels, the N that is retained or exported by the basin (snow N minus stream N) is shown in black, with positive values indicating a basin net "export" of N (hence gain to the stream) and negative values indicating a basin net "retention" of N (hence loss of N between the snowpack and stream). The third panel indicates the N-retention or N-export as a percent of the snowpack source of N.

To explore potential causes for N-retention or N-export, I regressed N-retention/export (kg-N ha^{-1}) on N_{snow} (snowpack N-loading) and on maximum basin-average SWE (Figure 14). I did not find a significant correlation between snowpack N-loading and N-retention/export. This may indicate that soil flushing may play a greater role in stream nitrate than the ionic pulse for

both GLV and TOK. Initially, I also did not find a significant relationship between maximum SWE and N-retention/export for the GLV4 or TOK. However, when the data points for GLV4 2002 and TOK 2003 were removed, I found significant ($p<0.05$) correlation between maximum SWE and N-retention/export for both GLV4 and TOK, with a positive correlation between these two variables for TOK (R^2 of 0.7225), and a negative correlation for GLV4 (R^2 of 0.51579) (Figure 14). In general for TOK, years with greater SWE exhibited N-export, and years with less SWE exhibited N-retention. Conversely, GLV4 exhibited decreasing amounts of N-export with increasing SWE accumulation. Of the 10 years of available data for TOK, 1996, 1997, 2002, and 2004 exhibited similar seasonal SWE accumulation (i.e. maximum basin SWE) of approximately 1.2 m. 1996 and 2002 exhibited N-export while 1997 and 2004 exhibited N-retention.

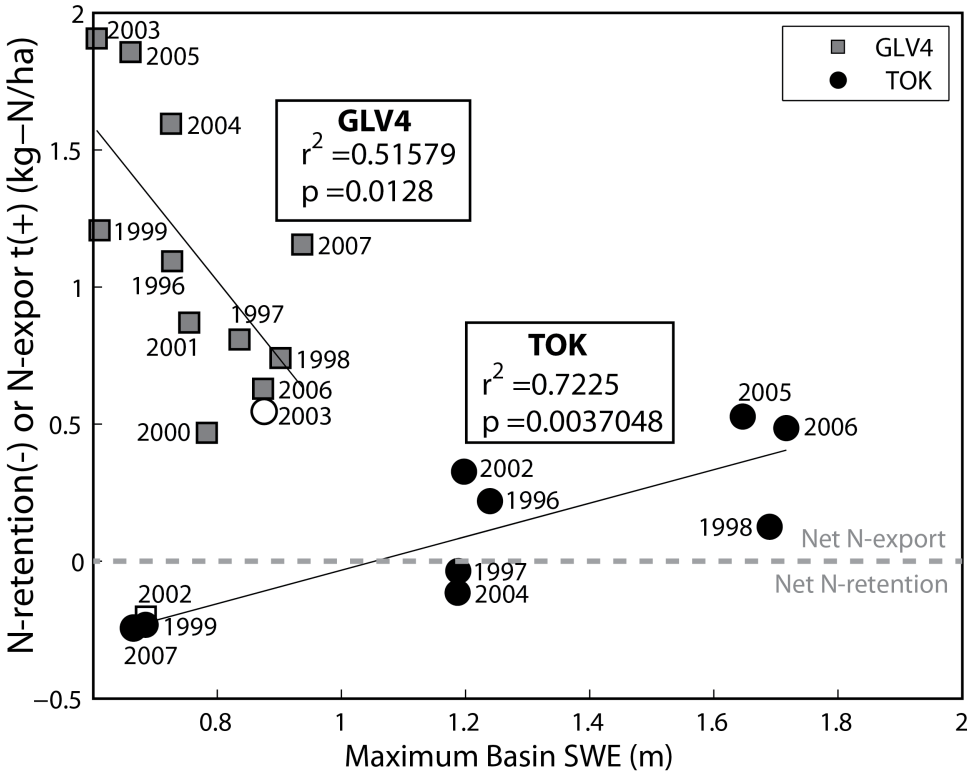

Figure 14. Maximum annual basin-average SWE versus N-retention/export for GLV4 and TOK. Removed outliers are shown as a white circle (TOK 2003) and white square (GLV4 2002).

6. DISCUSSION

The results indicate that GLV4 may be N-saturated, while TOK appears to exhibit N-retention and limitation. This is consistent with findings by previous studies [*Williams et al.*, 1996a; *Fenn et al.*, 1998; *Sickman et al.*, 2002]. Nitrate dynamics in these alpine ecosystems is controlled largely by microbial activity, which in turn is regulated by snow depth [*Brooks et al.*, 1996; *Brooks and Williams*, 1999]. Watersheds that are prone to wind scour and shallower snow depths (such as GLV4) are subject to lower rates of microbial activity, and thus are also prone to greater loss of nitrate from the soil during snowmelt [*Burns*, 2003]. In contrast, watersheds that are prone to deeper snow depths and more persistent snow cover have a greater potential for overwinter microbial activity, and thus are potentially subject to less flushing of inorganic N during snowmelt [*Burns*, 2003]. Of course, this is dependent on the availability of soil and talus that can host these microbial communities. GLV4 has higher microbial N-fixation potential as a function of soil/talus areas (62% of basin area) than TOK (47% of the basin area), and yet GLV4 exhibits 4.1 times more stream N-export than TOK. However, the snow depths on average for 1996-2007 were 25% greater in TOK than in GLV4, and 47% less spatially variable [*Jepsen et al.*, 2012]. A decreasing trend in the amount of net N_{snow}-export with an increase in maximum seasonal basin SWE in GLV4 is consistent with greater levels of microbial N-immobilization with an increase in snow depth [*Brooks et al.*, 1996]. This trend is reversed in TOK, with the basin exhibiting net N_{snow}-retention in years with a lower seasonal basin SWE and net N_{snow}-export in years with greater seasonal basin SWE (consistent with Sickman *et al.* 2002). It is likely that years with greater SWE in TOK have greater overwinter N-mineralization and nitrification in snow-covered soils, delayed growing seasons and reduced plant N-assimilation, and thus greater amounts of soil N available for flushing with the onset of snowmelt [*Sickman et*

al., 2002]. The interaction between max basin SWE and basin N-retention/saturation behavior was significant for both GLV4 and TOK, but it is likely that the difference in these relationships is a function of the surficial geology (rock/soil/talus areas) of each catchment [*Sickman et al.*, 2002].

GLV4 exhibited net N-export for all years except 2002, when it exhibited a net retention of N. In 2002, the basin exhibited a fairly high lag between the onset of snowmelt and peak discharge (~100 days), which was similar to the difference in the timing of the onset of snowmelt and peak stream nitrate concentration (also ~100 days). Peak discharge occurred within 20 days of the peak stream nitrate concentration. However, the peak stream nitrate concentration in 2002 was the lowest for all 12 years of measurement (~20 $\mu eq\ L^{-1}$). Additionally, the time constant (time it takes for the nitrate concentration to be reduced to 37% of its maximum value) was the greatest for 2002 of all of the 12 years of record (142 days, k = 0.007). This indicates that perhaps slower snowmelt allowed for greater opportunity for N-assimilation as meltwater slowly flushed from source areas to the stream. Another hypothesis is that slower snowmelt allowed for greater potential for deeper infiltration to deeper flowpaths, which reduced the amount of nitrate that could be flushed from the shallow subsurface. Additionally, in 2002, there was a negative correlation between NCA and stream nitrate ($r^2<0.5$); in other words, an increase in the "flushing" area of the cathment resulted in a decline in the stream nitrate concentration. This supports the hypothesis that there may not have been enough water pushed through the system to activate shallow flowpaths. 2002 was the fourth and worst year of drought in the Front Range, and it is possible that this water deficit influenced the nitrate-flushing dynamics that year. Basin flushing began on DOY 71, and ended on DOY 190 (119 days, which was fairly similar to the computed time constant). Flushing began first along the ridgetops on the exposed rocky outcrops

which are located furthest from the stream, and occurred approximately 20 days later on talus and soil (DOY 100). The last area of "flushing" was on the Arikaree Glacier. The rock glacier may play an important role in the elevated stream nitrate concentrations. In years with shallow snowpacks that melt earlier relative to other years, the rock glacier is exposed earlier and the ice may begin melting earlier. Because the rock glacier's meltwater contains high concentrations of nitrate, it may be that in years with low snow accumulation, the rock glacier may have higher contributions to stream nitrate [*Williams et al.*, 2007; *Baron et al.*, 2009].

Summer nitrate levels could also have been affected by summer precipitation, although I expect that this would result in nitrate pulses and not a constant stream nitrate concentration. From a preliminary analysis of monthly wet deposition collected at the Niwot Ridge Saddle NADP site for 1996-2004 (data not available for 2005, 2006, and 2007), I found that summer precipitation (June-Sept) was equivalent to precipitation amounts during the January-May period[2]. Summer nitrate loading (kg ha^{-1}) accounted for 6% less wet deposition than the January-May period on average (for 1996-2007). Although there was nearly as much contribution of nitrate loading in wet deposition during the summer as the winter, there were no notable spikes in stream nitrate from summer rain events. It is likely that these rain pulses do not contribute enough water to flush nitrate from the soil to the stream.

Although TOK was more variable in its peak stream nitrate timing, basin N-export/retention, and lag times, it exhibited less variable behavior in the relationship between NCA and the stream nitrate pulse. For all years of analysis in TOK (1996-2000, 2002-2007), there was a positive correlation between NCA and the stream nitrate concentration. Not only was the stream response to spatially-distributed snowmelt consistent, but NCA was a statistically-

[2] The NADP precipitation gage overcatches snowfall by approximately 61% [*Williams et al.*, 1998]. Snowfall precipitation values from January-May were scaled by 0.39 to account for this.

significant predictor of snowmelt; as much as 76% of the variability in the stream nitrate concentration could be explained by NCA. This signifies good hydraulic connectivity within TOK and VSA regulation in that the variability in the stream nitrate was related to the variability in the timing and distribution of snowmelt in the basin. Additionally, the best-correlated definition of NCA in TOK NCA9 (30 cm SWE loss). This is indicative that stream hydrochemistry in TOK could be sensitive not only to changes in the distribution and timing of snowmelt, but also to changes in the magnitude of snowmelt.

In contrast, GLV4 exhibited variability in its relationship between NCA and stream nitrate concentrations, despite less variability in the peak stream nitrate concentration, basin N-export, and lag times. GLV4 also exhibited a decreasing trend from 1996-2007 in nitrate flushing time constants (i.e. the amount of time it takes for the peak stream nitrate concentration to be reduced to 33% of its peak value) ($R^2 > 0.5$). This could be related to the general decreasing trend in maximum basin SWE in GLV4 from 1996-2007 [*Jepsen et al.*, 2012], and may suggest that GLV4 could potentially experience a continued decrease in nitrate flushing times with the potential decrease in SWE accumulation associated with a changing climate [*Mote*, 2006]. Still, the low correlation between the spatial distribution of snowmelt processes and the stream nitrate concentration supports that these processes are relatively decoupled in GLV4 due to deeper flowpaths that exist in the basin [*Liu et al.*, 2004; *Molotch et al.*, 2008].

To check whether snowmelt was consistently decoupled from stream nitrate dynamics in GLV4, I compared the timing of snowmelt (onset, median basin melt date), stream discharge, peak stream nitrate, and peak stream chloride (Figure 15). Chloride is a conservative hydrochemical tracer in that it accumulates in the seasonal snowpack and its signature is not affected by biogeochemical processes as meltwater travels from the source melting area to the

stream [*Williams et al.*, 1996c]. There were no notable chloride pulses in TOK during the snowmelt season. However, there were distinct annual spring chloride pulses observable in the outflow of GLV4. For several years (1996, 1997, 2004, 2005, and 2006), the timing of peak stream chloride concentrations were concurrent with the onset of snowmelt derived from the SWE reconstruction model, which is indicative of the ionic pulse of meltwater from the snowpack [*Bales et al.*, 1989]. In all years except 1996 and 1997, there was relatively little difference in the timing of flushing of exposed rock (ridgetops), talus, and soil (near the stream). In 1996, the timing of peak stream chloride was concurrent with the timing of melt for the exposed rock at the basin's ridgetops, and in 1997 snowmelt occurred over talus first and was concurrent with the peak stream chloride. This suggests that good hydraulic connectivity may exist between exposed rock and talus and the stream [*Liu et al.*, 2004] in GLV4, perhaps for years with deeper snowpacks when soils remain frozen but allow for overland flow of meltwater. Conversely, in 1998, 1999, 2000, 2001, 2002, and 2003, the stream Cl- pulse was delayed relative to the date of snowmelt onset. This may be a signature of the influence of longer and/or deeper subsurface flowpaths from the snowpack to the stream. Additionally, SWE accumulation was relatively low in these years, and the peak stream nitrate alternated year-to-year from higher to lower values. This alternating high/low nitrate concentration trend could potentially be the result of nitrate not fully flushing from flowpaths when subsurface flowpaths are relatively long or deep.

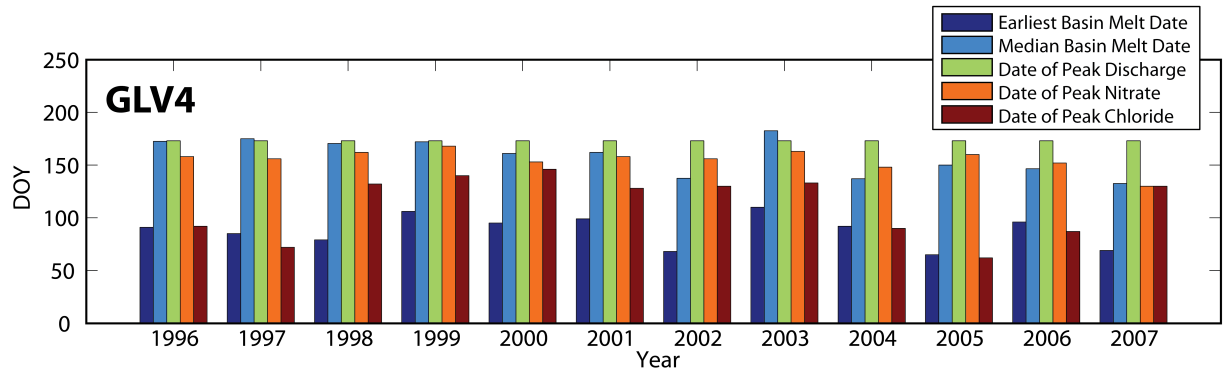

Figure 15. Earliest basin melt date, median basin melt date, date of peak discharge, date of peak stream nitrate concentration, and date of peak chloride concentration for GLV4, 1996-2007.

As a secondary check of the influence of snowpack dynamics on stream chemistry, I also regressed the number of melt pulse events per season on the peak stream nitrate concentrations for both GLV4 and TOK (Table 4). The melt pulse events were derived from the SWE reconstruction model and a threshold FSMA of 0.20. A basin melt pulse event was defined as any time FSMA exceeded and then fell below the threshold within a 3-day period. GLV4 experienced between 4 and 15 melt pulse events per season, and TOK experienced between 1 and 12 melt-pulse events per season (Table 3). The number of melt pulse events was not significantly correlated with the peak stream nitrate concentrations for either basin. I would expect that a greater number of melt pulse events would be correlated with a smaller magnitude stream nitrate pulse if stream nitrate was derived directly from snowmelt. No correlation confirms that in general, nitrate in snowpack meltwater likely interacts with chemical processes in soil or talus en route to the stream, which is consistent with previous studies in GLV4 and TOK [*Campbell et al.*, 1995; *Williams et al.*, 1996b; *Meixner et al.*, 2000; *Sickman et al.*, 2002; *Liu et al.*, 2004; *Molotch et al.*, 2008; *Cowie et al.*, 2011].

Table 4. Number of melt pulse events per snowmelt season for GLV4 and TOK.

	Number of Melt Pulse Events	
Year	**GLV4**	**TOK**
1996	12	7
1997	11	10
1998	15	11
1999	7	5
2000	7	9
2001	9	7
2002	8	1
2003	5	7
2004	10	4
2005	11	6
2006	4	4
2007	11	12

Although there was relatively low correlation between stream nitrate concentrations and NCA in GLV4, some years and some NCA definitions exhibited hysteresis (Figure 16), for which the falling limb of the nitrate pulse was highly correlated with a decline in NCA: initially, the stream nitrate concentration remained constant while NCA oscillated, until a specific day where the nitrate concentration increased dramatically with a very slight decrease in NCA, and then declined with a further decline in NCA. This was not observed in TOK. The nitrate concentrations in the stream were higher on the receding limb of NCA than on the rising limb.

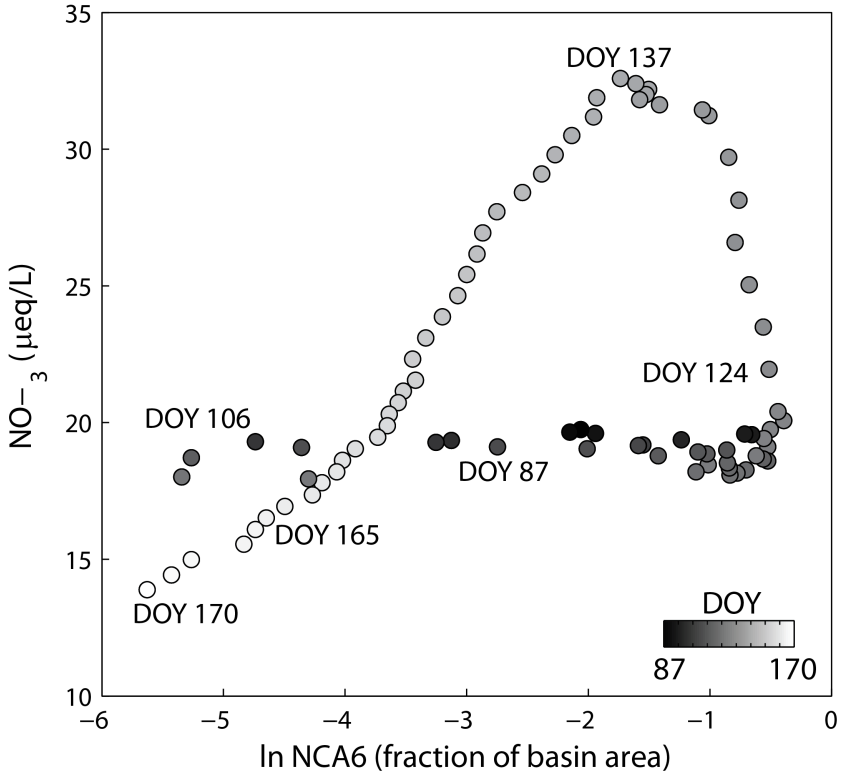

Figure 16. Hysteresis exhibited by some of the nitrate-NCA models. The example shown is GLV4 2006, NCA6 (50% melt of total initial SWE).

A possible conceptual model for explaining these hysteresis loops in GLV4 can be thought of as increasing basin hydraulic connectivity from the outside-in. For example, in GLV4 in 2006, NCA oscillated with constant stream nitrate concentrations until approximately DOY 123. From DOY 123 to 130, there is a steady linear increase in stream nitrate concentration with a decrease in the log of NCA. The basin exhibited a flushing pattern that started at the basin edges over rock subunits, and then progressed inward toward the basin outflow over soil and talus subunits, which should contain potentially greater pools of nitrate [*Williams et al.*, 1997]. Up until DOY 123, the basin experienced numerous MF cycles (i.e. short intermittent periods of melt), theoretically progressively increasing hydraulic connectivity in the basin until some critical amount on DOY 123. When this optimal hydraulic connectivity is reached, flowpaths

exist between the basin perimeter and the stream such that nitrate and water flushed first from the rock subunits can initiate flushing from the talus, which can then initiate flushing from the soil to the stream (Figure 17). This is the decrease in NCA that is observable in the hysteresis loop. The peak nitrate concentration does not occur at the peak NCA because it takes some amount of time (potentially one week, from DOY 123 to DOY 130) for water from the basin perimeter to reach the stream, and it may reach the stream at approximately the same time as when the nitrate from the talus and soil reaches the stream. In other words, areas may have already been "flushed" on a given day, but the flushed nitrate takes some amount of time to reach the stream as it flows through the saturated subsurface. While it may be intuitive that direct overland or shallow subsurface flowpaths to the basin outlet would be shorter for lower elevations and longer for the highest most distant reaches of the basin, it is more important to note the average flowpath length of various basin subunits relative to one another (Figure 17). The routing of water from one subunit to another (i.e. rock to talus to soil) provides a context for hypotheses regarding snowmelt-generation, hydrologic residence times, soil nitrate flushing, and stream discharge. Rather than VSA dynamics, these hysteresis loops suggest a new concept "declining" source area dynamics (DSA) for basins in which the hydrology is regulated by more complex flowpaths resulting from fractured bedrock and talus. We do not have data to support this hypothesis, but if this model applies to GLV4, then it is likely that an increase in soil moisture would be observable first near the basin perimeter and then would progress down toward the stream over some amount of time. Future work should be done to quantify the spatiotemporal distribution of soil moisture in GLV4 explore this hypothesis.

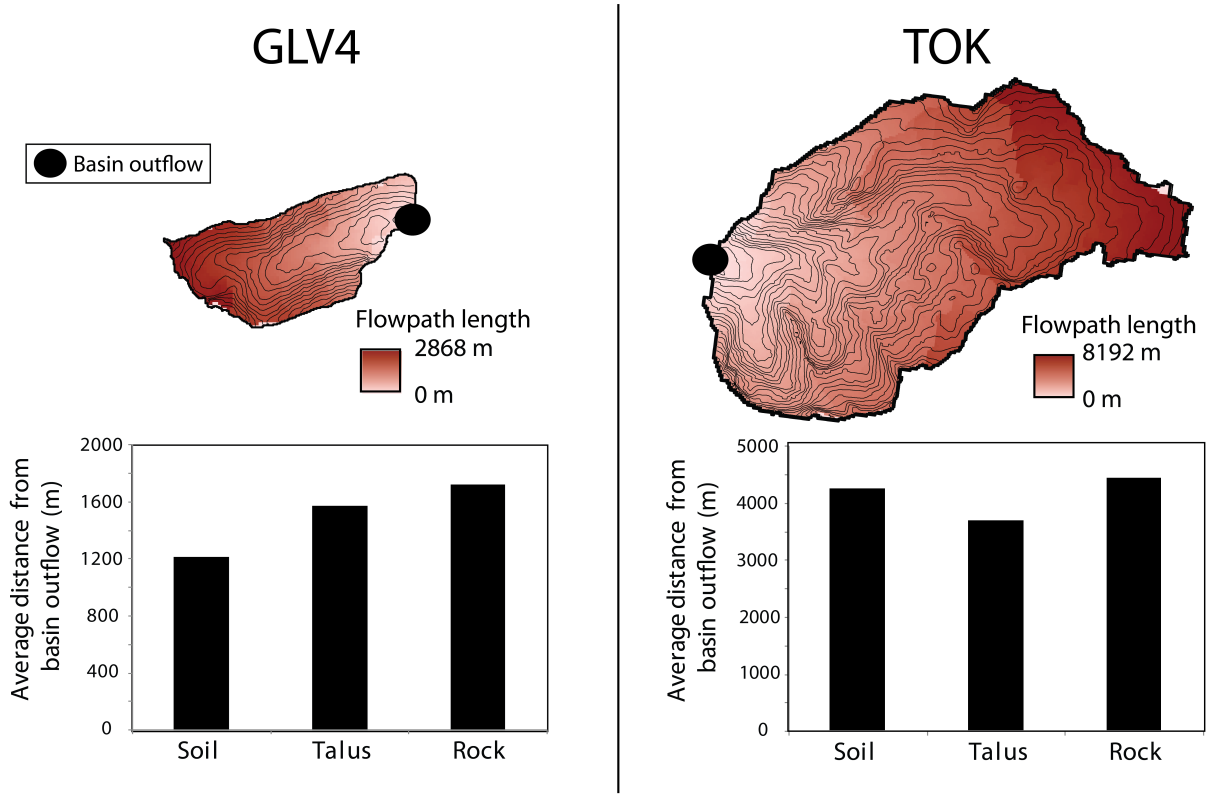

Figure 17. Maps and average distances from basin outflow along overland (and potentially shallow subsurface throughflow) flowpaths for basin subunits of soil, talus, and rock (30-m contour interval).

A variation of VSA dynamics could be at play in GLV4. Future research should focus on expanding this type of analysis to a larger number of seasonally snow covered basins that includes not only basins in the Rockies and Sierra Nevada, but also the Himalaya, Alps, and Andes to further explore the role of climate, glacial processes, and geology on basin hydrochemical responses. Future work should also examine the relationship between the spatiotemporal distribution of snowmelt and isotopes of N in the stream. This would allow for analysis of source waters to the stream for a better understanding water residence times, locations of deeper flowpaths, and importance of overwinter biogeochemical processes. These types of studies will become increasingly important for ecologic and water health monitoring and

water resources forecasting under changing and more variable climate regimes and increasing anthropogenic chemical impacts on alpine environments.

7. CONCLUSIONS

The primary goal of this study was to explore the applicability of a spatially distributed snowmelt model in explaining the nitrate dynamics of two geologically and climatologically dissimilar basins. Through correlation of stream nitrate with various definitions of NCA (i.e. areas of nitrate "flushing"), I found that on average, the modeled spatial distribution of new snowmelt explained 35% more variability in the stream nitrate in TOK than in GLV4. This stronger basin hydrochemical response to snowmelt indicates a potential sensitivity to changes in climate. Basins such as GLV4 may be better hydrochemically buffered to changes in climate and increases in N deposition due to deeper flowpaths that result in longer water residence time and greater opportunity for biologic assimilation of N. Still, GLV4 is already exhibiting N-saturation and increases in basin N-export associated with decreases in SWE accumulation. Although GLV4 may be relatively well buffered to changes in snowmelt, it may still be biogeochemically sensitive to changes in climate that may induce changes in SWE accumulation.

REFERENCES

Adam, J. C., A. F. Hamlet, and D. P. Lettenmaier (2009), Implications of global climate change for snowmelt hydrology in the twenty-first century, *Hydrol Process*, *23*(7), 962–972, doi:10.1002/hyp.7201.

Bales, R. C., N. P. Molotch, T. H. Painter, M. D. Dettinger, R. Rice, and J. Dozier (2006), Mountain hydrology of the western United States, *Water Resources Research*, *42*(8), W08432, doi:10.1029/2005WR004387.

Bales, R. C., R. E. Davis, and D. A. Stanley (1989), Ion elution through shallow homogeneous snow, *Water Resources Research*, *25*(8), 1869–1877.

Barnett, T. P., J. C. Adam, and D. P. Lettenmaier (2005), Potential impacts of a warming climate on water availability in snow-dominated regions, *Nature*, *438*(7066), 303–309, doi:10.1038/nature04141.

Baron, J. S., D. S. Ojima, E. A. Holland, and W. J. Parton (1994), Analysis of nitrogen saturation potential in Rocky Mountain tundra and forest: implications for aquatic systems, *Biogeochemistry*, *27*(1), 61–82.

Baron, J. S., T. M. Schmidt, and M. D. Hartman (2009), Climate-induced changes in high elevation stream nitrate dynamics, *Global Change Biology*, *15*(7), 1777–1789.

Brooks, P. D., and M. W. Williams (1999), Snowpack controls on nitrogen cycling and export in seasonally snow-covered catchments, *Hydrol Process*, *13*, 2177–2190.

Brooks, P. D., M. W. Williams, and S. K. Schmidt (1996), Microbial activity under alpine snowpacks, Niwot Ridge, Colorado, *Biogeochemistry*, *32*(2), 93–113.

Burns, D. A. (2003), The effects of atmospheric nitrogen deposition in the Rocky Mountains of Colorado and southern Wyoming, USA- a critical review, *Environmental Pollution*, *127*, 257–269, doi:10.1016/S0269-7491(03)00264-1.

Butcher, S.S., R.J. Charlson, G.H. Orians, G.V. Wolfe (eds.) (1992), Global Biogeochemical Cycles, 379 pp., Academic Press, San Diego.

Caine, N. (1995), Temporal trends in the quality of streamwater in an alpine environment: Green Lakes Valley, Colorado Front Range, USA, *Geografiska Annaler. Series A. Physical Geography*, 207–220.

Caine, N., and E. M. Thurman (1990), Temporal and spatial variations in the solute content of an alpine stream, Colorado Front Range, *Geomorphology*, *4*(1), 55–72, doi:10.1016/0169-555X(90)90026-M.

Campbell, D. H., D. W. Clow, G. P. Ingersoll, M. A. Mast, N. E. Spahr, and J. T. Turk (1995), Processes controlling the chemistry of two snowmelt-dominated streams in the Rocky Mountains, *Water Resources Research*, *31*(11), 2811–2821.

Cline, D. W., R. C. Bales, and J. Dozier (1998), Estimating the spatial distribution of snow in mountain basins using remote sensing and energy balance modeling, *Water Resources Research*, *34*, 1275–1285.

Cowie, R., M. W. Williams, N. Caine, and R. Michel (2011), Estimated residence time of two snowmelt dominated catchments, Boulder Creek watershed, Colorado, *Proceedings of the Western Snow Conference*, *3*(10), 1–8.

Creed, I. F., and L. E. Band (1998), Export of nitrogen from catchments within a temperate forest: Evidence for a unifying mechanism regulated by variable source area dynamics, *Water Resources Research*, *34*(11), 3105, doi:10.1029/98WR01924.

Dise, N. B., and R. F. Wright (1995), Nitrogen leaching from European forests in relation to nitrogen deposition, *Forest Ecology and Management*, *71*(1-2), 153–161, doi:10.1016/0378-1127(94)06092-W.

Erickson, T. A., M. W. Williams, and A. Winstral (2005), Persistence of topographic controls on the spatial distribution of snow in rugged mountain terrain, Colorado, United States, *Water Resources Research*, *41*(4), W04014–, doi:10.1029/2003WR002973.

Fenn, M. E. et al. (2003), Nitrogen Emissions, Deposition, and Monitoring in the Western United States, *BioScience*, *53*(4), 391–403.

Fenn, M. E., M. A. Poth, J. D. Aber, J. S. Baron, B. T. Bormann, D. W. Johnson, A. D. Lemly, S. G. McNulty, D. F. Ryan, and R. Stottlemyer (1998), Nitrogen excess in North American ecosystems: Predisposing factors, ecosystem responses, and management strategies, *Ecological Applications*, *8*(3), 706–733, doi:10.1890/1051-0761(1998)008[0706:NEINAE]2.0.CO;2.

Galloway, J. N., J. D. Aber, J. W. Erisman, S. P. Seitzinger, R. W. Howarth, E. B. Cowling, and B. J. Cosby (2003), The Nitrogen cascade, *BioScience*, *53*(4), 341, doi:10.1641/0006-3568(2003)053[0341:TNC]2.0.CO;2.

Gruber, N., and J. N. Galloway (2008), An Earth-system perspective of the global nitrogen cycle, *Nature*, *451*(7176), 293–296, doi:doi:10.1038/nature06592.

Harrington, R., and R. C. Bales (1998), Modeling ionic solute transport in melting snow, *Water Resources Research*, *34*, 1727–1736.

Heuer, K., P. D. Brooks, and K. A. Tonnessen (1999), Nitrogen dynamics in two high elevation catchments during spring snowmelt 1996, Rocky Mountains, Colorado, *Hydrol Process*, *13*(14-15), 2203–2214.

Jepsen, S. M., N. P. Molotch, M. W. Williams, K. E. Rittger, and J. O. Sickman (2012), Interannual variability of snowmelt in the Sierra Nevada and Rocky Mountains, United States: Examples from two alpine watersheds, *Water Resources Research*, *48*(2), W02529, doi:10.1029/2011WR011006.

Johannessen, M., and A. Henriksen (1978), Chemistry of Snow Meltwater - Changes in Concentration During Melting, *Water Resources Research*, *14*(4), 615–619.

Kapnick, S., and A. Hall (2010), Observed Climate-Snowpack Relationships in California and their Implications for the Future, *J Climate*, *23*(13), 3446–3456, doi:10.1175/2010JCLI2903.1.

Ley, R. E., M. W. Williams, and S. K. Schmidt (2004), Microbial population dynamics in an extreme environment: controlling factors in talus soils at 3750 m in the Colorado Rocky Mountains, *Biogeochemistry*, *68*(3), 297–311.

Liu, F., M. W. Williams, and N. Caine (2004), Source waters and flow paths in an alpine catchment, Colorado Front Range, United States, *Water Resources Research*, *40*(9), W09401, doi:10.1029/2004WR003076.

Magnusson, J., T. Jonas, I. Lopez-Moreno, and M. Lehning (2010), Snow cover response to climate change in a high alpine and half-glacierized basin in Switzerland, *Hydrology research*, *41*(3-4), 230–240.

Marks, D., J. Domingo, D. Susong, T. Link, and D. Garen (1999), A spatially distributed energy balance snowmelt model for application in mountain basins, *Hydrol Process*, *13*(1213), 1935–1959.

Marks, D., J. Dozier, and R. E. Davis (1992), Climate and energy exchange at the snow surface in the alpine region of the Sierra Nevada, *Water Resources Research*, *28*(11), 3043–3054.

Martinec, J., and A. Rango (1981), Areal distribution of snow water equivalent evaluated by snow cover monitoring, *Water Resources Research*.

McClain, M. E. et al. (2003), Biogeochemical Hot Spots and Hot Moments at the interface of terrestrial and aquatic ecosystems, *Ecosystems*, *6*(4), 301–312, doi:10.1007/s10021-003-0161-9.

McDonnell, J. J. (2009), Hewlett, J.D. and Hibbert, A.R. 1967: Factors affecting the response of small watersheds to precipitation in humid areas. In Sopper, W.E. and Lull, H.W., editors, Forest hydrology, New York: Pergamon Press, 275--90, *Progress in Physical Geography*, *33*(2), 288–293, doi:10.1177/0309133309338118.

Meixner, T., R. C. Bales, M. W. Williams, D. H. Campbell, and J. S. Baron (2000), Stream chemistry modeling of two watersheds in the Front Range, Colorado, *Water Resources Research*, *36*(1), 77–87, doi:10.1029/1999WR900248.

Molotch, N. P. (2009), Reconstructing snow water equivalent in the Rio Grande headwaters using remotely sensed snow cover data and a spatially distributed snowmelt model, edited by C. de Jong, D. Lawler, and R. Essery, *Hydrol Process*, *23*(7), 1076–1089, doi:10.1002/hyp.7206.

Molotch, N. P., and R. C. Bales (2006), Comparison of ground-based and airborne snow surface

albedo parameterizations in an alpine watershed: Impact on snowpack mass balance, *Water Resources Research*, *42*(5), W05410–, doi:10.1029/2005WR004522.

Molotch, N. P., and S. A. Margulis (2008), Estimating the distribution of snow water equivalent using remotely sensed snow cover data and a spatially distributed snowmelt model: A multi-resolution, multi-sensor comparison, *Advances in Water Resources*, *31*(11), 1503–1514.

Molotch, N. P., T. H. Painter, R. C. Bales, and J. Dozier (2004), Incorporating remotely-sensed snow albedo into a spatially-distributed snowmelt model, *Geophys. Res. Lett.*, *31*(3), L03501, doi:10.1029/2003GL019063.

Molotch, N. P., T. Meixner, and M. W. Williams (2008), Estimating stream chemistry during the snowmelt pulse using a spatially distributed, coupled snowmelt and hydrochemical modeling approach, *Water Resources Research*, *44*(11), W11429.

Mote, P. W. (2006), Climate-driven variability and trends in mountain snowpack in western North America, *J Climate*, *19*(23), 6209–6220.

Painter, T. H., J. Dozier, D. A. Roberts, R. E. Davis, and R. O. Green (2003), Retrieval of subpixel snow-covered area and grain size from imaging spectrometer data, *Remote Sensing of Environment*, *85*(1), 64–77, doi:10.1016/S0034-4257(02)00187-6.

Painter, T. H., K. Rittger, C. McKenzie, P. Slaughter, R. E. Davis, and J. Dozier (2009), Retrieval of subpixel snow covered area, grain size, and albedo from MODIS, *Remote Sensing of Environment*, *113*(4), 868–879.

Rascher, C. M., C. T. Driscoll, and N. E. Peters (1987), Concentration and flux of solutes from snow and forest floor during snowmelt in the West-Central Adirondack region of New York, *Biogeochemistry*, *3*(1), 209–224.

Ross A Wolford, R. C. B. S. S. (2007), Development of a hydrochemical model for seasonally snow-covered alpine watersheds: Application to Emerald Lake watershed, Sierra Nevada, California, *Water Resources Research*, *32*(4), 1061–1074. [online] Available from: http://www.agu.org/journals/wr/v032/i004/95WR03726/95WR03726.pdf

Sickman, J. O., A. Leydecker, and J. M. Melack (2001), Nitrogen mass balances and abiotic controls on N retention and yield in high-elevation catchments of the Sierra Nevada, California, United States, *Water Resources Research*, *37*(5), 1445–1461.

Sickman, J. O., J. M. Melack, and J. L. Stoddard (2002), Regional analysis of inorganic nitrogen yield and retention in high-elevation ecosystems of the Sierra Nevada and Rocky Mountains, *Biogeochemistry*, *57*(1), 341–374.

Tonnessen, K. A. (1991), The Emerald Lake watershed study: Introduction and site description, *Water Resources Research*, *27*, 1537–1539.

Tsiouris, S., C. E. Vincent, T. D. Davies, and P. Brimblecombe (1985), The elution of ions through field and laboratory snowpacks, *Ann Glaciol*.

Wagener, T., M. Sivapalan, P. A. Troch, B. L. McGlynn, C. J. Harman, H. V. Gupta, P. Kumar, P. S. C. Rao, N. B. Basu, and J. S. Wilson (2010), The future of hydrology: An evolving science for a changing world, *Water Resources Research*, *46*(5), W05301, doi:10.1029/2009WR008906.

Wetzel, R.G. (1983), Limnology, 2nd Edition, 766 pp., Saunders College Publishing, United States of America.

Williams, M. W., A. D. Brown, and J. M. Melack (1993), Geochemical and hydrologic controls on the composition of surface water in a high-elevation basin, Sierra Nevada, California, *Limnol Oceanogr*, *38*(4), 775–797.

Williams, M. W., and J. M. Melack (1991a), Precipitation chemistry in and ionic loading to an alpine basin, Sierra Nevada, *Water Resources Research*, *27*, 1563–1574.

Williams, M. W., and J. M. Melack (1991b), Solute chemistry of snowmelt and runoff in an alpine basin, Sierra Nevada, *Water Resources Research*, *27*(7), 1575–1588.

Williams, M. W., and K. A. Tonnessen (2000), Critical loads for inorganic nitrogen deposition in the Colorado Front Range, USA, *Ecological Applications*, *10*(6), 1648–1665, doi:10.1890/1051-0761(2000)010[1648:CLFIND]2.0.CO;2.

Williams, M. W., J. S. Baron, N. Caine, R. Sommerfeld, and R. Sanford (1996a), Nitrogen saturation in the Rocky Mountains, *Environ. Sci. Technol.*, *30*(2), 640–646, doi:10.1021/es950383e.

Williams, M. W., M. Knauf, N. Caine, F. Liu, and P. L. Verplanck (2006), Geochemistry and source waters of rock glacier outflow, Colorado Front Range, *Permafrost Periglac. Process.*, *17*(1), 13–33, doi:10.1002/ppp.535.

Williams, M. W., M. Knauf, R. Cory, N. Caine, and F. Liu (2007), Nitrate content and potential microbial signature of rock glacier outflow, Colorado Front Range, *Earth Surf. Process. Landforms*, *32*(7), 1032–1047, doi:10.1002/esp.1455.

Williams, M. W., M. Losleben, N. Caine, and D. Greenland (1996b), Changes in climate and hydrochemical responses in a high-elevation catchment in the Rocky Mountains, USA, vol. 41, pp. 939–946.

Williams, M. W., P. D. Brooks, A. Mosier, and K. A. Tonnessen (1996c), Mineral nitrogen transformations in and under seasonal snow in a high-elevation catchment in the Rocky Mountains, United States, *Water Resources Research*, *32*(10), 3161, doi:10.1029/96WR02240.

Williams, M. W., T. Bardsley, and M. Rikkers (1998), Overestimation of snow depth and inorganic nitrogen wetfall using NADP data, Niwot Ridge, Colorado, *Atmospheric Environment*, *32*, 3827–3833.

Williams, M. W., T. Davinroy, and P. D. Brooks (1997), Organic and inorganic nitrogen pools in

talus fields and subtalus water, Green Lakes Valley, Colorado Front Range, *Hydrol Process*, *11*(13), 1747–1760.

Wolford, R. A., R. C. Bales, and S. Sorooshian (1996), Development of a Hydrochemical Model for Seasonally Snow-Covered Alpine Watersheds: Application to Emerald Lake Watershed, Sierra Nevada, California,, *32*, 1061–1074.